

# **Biotin and boron-dipyrromethene tagged platinum(IV) prodrug for cellular imaging and mito-targeted photocytotoxicity in red light**

Arpan Bera,<sup>a</sup> Amrita Nepalia,<sup>b</sup> Aarti Upadhyay,<sup>a</sup> Deepak Kumar Saini,<sup>\*b</sup> and Akhil R. Chakravarty<sup>\*a</sup>

<sup>a</sup> *Department of Inorganic and Physical Chemistry, Indian Institute of Science, Sir C.V. Raman Avenue, Bangalore 560012, India. E-mail: [arc@iisc.ac.in](mailto:arc@iisc.ac.in)*

<sup>b</sup> *Department of Molecular Reproduction, Development and Genetics, Indian Institute of Science, Bangalore 560012, India. E-mail: [deepaksaini@iisc.ac.in](mailto:deepaksaini@iisc.ac.in)*

**Electronic Supplementary Information (ESI)**

# Table of contents

## General information and methods

*Materials and methods*

*Instrumentation*

*Singlet oxygen quantum yield determination*

*Theoretical calculations*

*DNA photocleavage studies*

*MTT assay*

*Confocal microscopy*

*DCFDA assay*

*JC-1 assay*

*Annexin V-FITC/Propidium Iodide assay*

*$\beta$ -Tubulin immunostaining assay*

**Scheme S1.** Scheme for the synthesis of precursor **A**. TFA is trifluoroacetic acid and DCM is dichloromethane.

**Scheme S2.** Scheme for the synthesis of Me-L.

**Scheme S3.** Scheme for the synthesis of HL. THF is tetrahydrofuran.

**Fig. S1.**  $^1\text{H}$  NMR spectrum of ligand precursor Me-L in  $\text{CDCl}_3$ .

**Fig. S2.**  $^1\text{H}$  NMR spectrum of ligand HL in  $\text{CDCl}_3$ .

**Fig. S3.**  $^1\text{H}$  NMR spectrum of complex **1** in  $\text{DMSO-d}_6$ . The metal-bound ammine 6H peaks appeared broad.

**Fig. S4.**  $^{13}\text{C}$  NMR spectrum of Me-L in  $\text{CDCl}_3$ .

**Fig. S5.**  $^{13}\text{C}$  NMR spectrum of HL in  $\text{CDCl}_3$ .

**Fig. S6.**  $^{13}\text{C}$  NMR spectrum of complex **1** in  $\text{DMSO-d}_6$ .

**Fig. S7.**  $^{11}\text{B}$  NMR spectrum of Me-L in  $\text{CDCl}_3$ .

**Fig. S8.**  $^{11}\text{B}$  NMR spectrum of HL in  $\text{CDCl}_3$ .

**Fig. S9.**  $^{11}\text{B}$  NMR spectrum of complex **1** in  $\text{DMSO-d}_6$ .

**Fig. S10.** Mass spectrum of Me-L recorded in acetonitrile with a peak corresponding to  $[\text{M}+\text{Na}]^+$  (m/z) at 905.4011.

**Fig. S11.** Mass spectrum of HL recorded in acetonitrile with a peak corresponding to  $[M+Na]^+$  ( $m/z$ ) at 891.3850.

**Fig. S12.** (a) Mass spectrum of complex **1** recorded in acetonitrile with a peak corresponding to  $[M+Na]^+$  ( $m/z$ ) at 1433.4166. (b) Isotopic distribution of the complex showing the presence of platinum. (c) Simulated isotopic distribution pattern.

**Fig. S13.** UV-visible spectra of complex **1** recorded at different concentration in DMSO, and absorbance was plotted against the concentration.

**Fig. S14.** Fluorescence quantum yield for ligand HL in DMSO.

**Fig. S15.** Fluorescence quantum yield for complex **1** in DMSO.

**Fig. S16.** Cyclic voltammogram of complex **1** at 10% aqueous DMF at  $100 \text{ mV s}^{-1}$ .

**Fig. S17.** (a) Optimized geometry of the *cis,cis,trans*-Pt(IV) complex **1** as obtained from the quantum calculations using B3LYP/LanL2DZ level of theory. The six-coordinate geometry has a cisplatin basal plane and two axial ligands having biotin and a BODIPY moiety. (b) Nodal patterns of HOMO and LUMO as generated from the optimized structure.

**Fig. S18.** Time-dependent stability studies of complex **1** in 1:1 (v/v) DMSO/DPBS (pH = 7.4) under dark condition. It shows no major spectral changes over time and the spectral features remained essentially the same.

**Fig. S19.** Time-dependent stability studies of complex **1** in 1:1 (v/v) DMSO/DPBS under dark condition at different pH condition: (a) pH = 3.0 and (b) pH = 9.0.

**Fig. S20.** (a) Increase in emission intensity of Pt(IV) complex **1** in 1:1 (v/v) DMSO/DPBS ( $\lambda_{\text{ex}} = 630 \text{ nm}$ ) upon red light (642 nm laser) irradiation suggesting possible release of the emissive BODIPY ligand. The traces were taken up to 5 min. (b) Emission intensity of the complex remained unaltered under dark conditions indicating its high dark stability. Data were recorded up to 120 min in the dark.

**Fig. S21.** (a) ESI-MS of light-exposed complex **1** solution (used for NMR study). The 349.0340 peak is assignable to species formulated as  $[\text{Pt}(\text{NH}_3)_2\text{Cl}(\text{DMSO-d}_6)]^+$ , 245.0951 and 891.3850 peaks are due to free biotin and BODIPY ligand respectively released from the complex after light irradiation. (b) Isotopic distribution of  $[\text{Pt}(\text{NH}_3)_2\text{Cl}(\text{DMSO-d}_6)]^+$  adduct with the inset showing the simulated isotopic distribution indicating the presence of platinum.

**Fig. S22.** (a) ESI-MS study of DNA binding ability of light exposed solution with model nucleobase 9-ethylguanine (9-EtG). Experiment was performed by taking light exposed sample with 4 equiv. 9-EtG after 6 h of incubation. The peak corresponding to 444.0810  $m/z$  suggests the formation of the species  $[\text{Pt}(\text{NH}_3)_2\text{Cl}(9\text{-EtG})]^+$ . (b) Isotopic distribution pattern of  $[\text{Pt}(\text{NH}_3)_2\text{Cl}(9\text{-EtG})]^+$  and the inset shows the simulated isotopic distribution pattern indicating the presence of platinum and overall one charge of the complex.

**Fig. S23.** (a) Ethidium bromide (EB) assay showing a decrease in the emission intensity indicating DNA crosslink formation upon light irradiation. A decrease in the emission intensity of EB (50  $\mu\text{M}$ ) at 605 nm was observed when the ct-DNA and complex **1** (30  $\mu\text{M}$ ) containing solution was photo irradiated. (b) Emission intensity of EB remained the same in dark for over 40 min period.

**Fig. S24.** Time-dependent  $^1\text{H}$  NMR spectra of complex **1** in presence of 10 equiv. ascorbic acid as a reducing agent. The signal for six ammine protons (marked with blue diamond motif) disappeared on

metal reduction from Pt(IV) to Pt(II) in presence of ascorbic acid as a reducing agent thus releasing the ligand HL and biotin. Broad peaks near 8.3 ppm and 4.4 ppm are due to ascorbic acid.

**Fig. S25.** Changes in the absorption spectra of DBBF containing ligand HL (50:1 concentration ratio) on red light exposure (642 nm, 100 mW) in DMSO.

**Fig. S26.**  $\Delta$ OD vs. irradiation time for determining singlet oxygen quantum yield ( $\Phi_{\Delta}$ ) of complex **1** and HL (MB, methylene blue used as a control). The plot shows the importance of platinum for the high  $\Phi_{\Delta}$  value of complex **1** compared to the ligand HL alone.

**Fig. S27.** (a) Gel diagram showing photocleavage of pUC19 DNA (33  $\mu$ M) in presence of complex **1** (30  $\mu$ M) upon 642 nm red laser irradiation for 45 min duration. Lanes are: (1) DNA control (in light) showing SC form only, (2) DNA + complex **1** (in light) showing essential formation of NC form from SC form, (3) DNA + complex **1** (in dark) showing SC form. Lanes (4-11) are showing mechanistic aspects of the photocleavage of pUC19 DNA in presence of complex **1** and different scavengers/quenchers/additives, namely, KI, 6  $\mu$ M; TEMP, 6  $\mu$ M; NaN<sub>3</sub>, 6  $\mu$ M; DHN, 6  $\mu$ M; DMSO, 4  $\mu$ L; SOD, 4 units; catalase, 4 units; Tiron, 6  $\mu$ M using red laser light (642 nm) irradiation. Lanes are: (4) DNA + complex **1** + NaN<sub>3</sub> (showing quenching), (5) DNA + complex **1** + TEMP (showing partial quenching), (6) DNA + complex **1** + DHN (1,5-dihydroxynaphthalene) (showing quenching), (7) DNA + complex **1** + KI, (8) DNA + complex **1** + DMSO, (9) DNA + complex **1** + catalase, (10) DNA + complex **1** + Tiron, and (11) DNA + complex **1** + SOD. Lanes 7-11 show no apparent scavenging effect of the reagents added giving %NC within 75-83% which is similar to 85% of NC DNA formed (lane 2).

**Fig. S28.** Cell viability plots obtained from MTT assay of complex **1** in A549 cells on light exposure (L, 600-720 nm, 20 min exposure, light dose: 30 J cm<sup>-2</sup>) and in dark (D) condition.

**Fig. S29.** Cell viability plots obtained from MTT assay of complex **1** in MDA-MB-231 cells on light exposure (L, 600-720 nm, 20 min exposure, light dose: 30 J cm<sup>-2</sup>) and in dark (D) condition.

**Fig. S30.** Cell viability plots obtained from MTT assay of ligand HL in A549 cells on light exposure (L, 600-720 nm, 20 min exposure, light dose: 30 Joules cm<sup>-2</sup>) and in dark (D) condition.

**Fig. S31.** Cell viability plots obtained from MTT assay of ligand HL in MDA-MB-231 cells on light exposure (L, 600-720 nm, 20 min exposure, light dose: 30 Joules cm<sup>-2</sup>) and in dark (D) condition.

**Fig. S32.** Cell viability plots obtained from MTT assay of complex **1** in Beas-2B cells on light exposure (L, 600-720 nm, 20 min exposure, light dose: 30 Joules cm<sup>-2</sup>) and in dark (D) condition.

**Fig. S33.** Cell viability plots obtained from MTT assay of ligand HL in Beas-2B cells on light exposure (L, 600-720 nm, 20 min exposure, light dose: 30 Joules cm<sup>-2</sup>) and in dark (D) condition.

**Fig. S34.** Cell viability plots obtained from MTT assay of cisplatin in A549 cells on light exposure (L, 600-720 nm, 20 min exposure, light dose: 30 Joules cm<sup>-2</sup>) and in dark (D) condition.

**Fig. S35.** Confocal images of A549 cells incubated with complex **1**. The panels are: (i) complex **1**-based emission (ii) green emitting ER tracker (ERG) (iii) bright field (iv) merged image without bright field (v) merged image with bright field. Scale bar 20  $\mu$ m.

**Fig. S36.** Immunofluorescence study to investigate the impact of light treatments on the microtubule network of the complex treated A549 cells. Microtubules were visualized with  $\beta$ -tubulin antibody interacting with a secondary antibody tagged with Alexa Fluor 488. Panels are: (i) untreated cells, (ii) dark set, and (iii) light set. Apoptotic bodies are marked with yellow arrows in panel (iii).

**Table S1.** Coordinates of optimized geometry for complex **1** obtained from DFT using B3LYP/LanL2DZ level of theory for all atoms.

**Table S2.** Excitation energies and oscillator strengths obtained from TD-DFT calculations for complex **1**.

## Materials and methods

All the reagents and chemicals were purchased from commercial sources and used without further purification. Dry DMF was purchased from Spectrochem, India and other solvents were purchased from SD Fine Chem Ltd. and Avra (India). Cisplatin was purchased from Arora Matthey Ltd. (India) and converted to **Oxoplatin** by following a published procedure. Dichloromethane and toluene were dried over P<sub>2</sub>O<sub>5</sub> and sodium, respectively. All the reactions were performed under ambient temperature and pressure unless otherwise mentioned. Chemicals for biological assays, cell culture media and buffer were purchased from Thermo Fisher Scientific (Invitrogen) and Sigma Aldrich. Supercoiled plasmid DNA (pUC19) was procured from Genie, Bangalore (India).

## Instrumentation

<sup>1</sup>H and other multinuclear NMR spectral studies were performed using Bruker Avance 400 MHz and Bruker Ascend 500 MHz NMR spectrometers and data analysis was performed using topspin 3.6.2 software with trimethylsilane (TMS) as an internal standard ( $\delta = 0.0$  ppm). Mass spectral analysis was performed in Agilent 6538 ultra-high definition (UHD) accurate mass Q-TOF spectrometer. Simulation of isotopic distribution pattern was performed by molecular weight calculator software. Elemental analysis was performed by Thermo Scientific Flash 2000 Organic Elemental Analyzer. For molar conductivity measurements a control dynamics conductivity meter was used. For electrochemical experiment, an EG&G PAR model 253 VersaStat potentiostat/galvanostat with EZchem electrochemical analysis software and three electrodes set up having a glassy carbon working, platinum wire as auxiliary and saturated calomel reference electrode (SCE) and 0.1 M tetrabutylammonium hexafluorophosphate (TBAHP) as supporting electrolyte was used. Absorption spectra were recorded using a PerkinElmer Shimadzu UV-2600 spectrophotometers and emission spectra were recorded using a HORIBA JOBIN YVON FluoroMax-4 and HORIBA Duetta Spectrometer. For MTT assay absorbance at 570 nm was recorded using TECAN microplate reader and IC<sub>50</sub> values were estimated by nonlinear regression analysis (Graph Pad Prism 8) software. Confocal images were recorded using Zeiss LSM 880 microscope. Flow cytometric analysis was done

using FACS VERSE (BD FACS) software and data analysis was done using FACS suite and FCS express 7 software.

### **Singlet oxygen quantum yield determination**

Singlet oxygen quantum yield was determined from 1,3-diphenylisobenzofuran (DPBF) titration experiment. It acted as a singlet oxygen scavenger which reacts with singlet oxygen to form 1,2-dibenzoylbenzene. Complex **1** and ligand **HL** were dissolved in 50:1 molar concentration ratio in DMSO and shined with 642 nm laser source. Photooxidation of DPBF was monitored by decrease in absorbance maxima at 417 nm at 3 sec time intervals. For quantum yield determination, methylene blue ( $\Phi_{\Delta} = 0.52$ ) was used as a standard. A decrease in the DPBF absorption maxima intensity around 417 nm was plotted against the irradiation time. The singlet oxygen quantum yield values ( $\Phi_{\Delta}$ ) were obtained by using following equation:

$$\Phi_{\Delta C} = \Phi_{\Delta MB} \times (m_C/m_{MB}) \times (F_{MB}/F_C) \dots (1)$$

where, subscript “C” refers to complex **1** and ligand **HL** and subscript “MB” refers to methylene blue,  $\Phi_{\Delta}$  is the value of singlet oxygen quantum yield, m is the slope of  $\Delta OD$  vs. time plot and “F” is the absorption correction factor. It can be expressed as  $F = 1 - 10^{-OD}$ , where OD is the optical density (absorbance) at irradiation wavelength.

### **Theoretical calculations**

All the DFT optimizations were performed with Gaussian 16 package using B3LYP level of theory and LanL2DZ (Los Alamos National Laboratory 2 Double-Zeta) basis set for all atoms. Time-dependent density functional theory calculations were carried out to obtain possible electronic transitions. Calculations were done using LanL2DZ basis set with B3LYP level of theory. Bulk solvent effect of DMSO was included through IEF-PCM model. Nodal patterns of HOMO and LUMO were plotted using Chemcraft software.<sup>S1,S2</sup>

### **DNA photocleavage studies**

Photoinduced DNA cleavage of pUC19 DNA (33  $\mu$ M) by complex (30  $\mu$ M) was studied by gel-electrophoresis method in 10% DMF/tris-HCl buffer medium at pH = 7.2. Photoirradiation of the sample was carried out with 642 nm laser source (power 100 mW) for 20 min. For the experiment, the sample was prepared by adding 1  $\mu$ l of SC DNA, 50 mM of NaCl, complex **1** and Tris-HCl buffer. Samples were kept for 1 h incubation at 37 °C before light exposure. After

20 min of light irradiation each sample was treated with 2  $\mu$ l of loading dye (0.25 % bromophenol blue, 0.25 % xylene cyanol, 30 % glycerol) was added. Around 0.17 g of agarose type-I was melted in 20 ml of 1 buffer and then 5  $\mu$ l of ethidium bromide was added and the mixture was poured in a gel casting tray and allowed to cool at room temperature for about ~40 min. Each sample was then loaded on agarose gel. Electrophoresis was carried out in a dark chamber for 2 h at 60 V in TAE buffer. Mechanistic investigations to identify the nature of ROS produced were done in presence of different ROS quenchers/scavengers, namely, sodium azide ( $\text{NaN}_3$ ), 2,2,6,6-tetramethyl-4-piperidone (TEMP), 1,5 -dihydroxy-naphthalene (DHN) as singlet oxygen quencher. The amount of % NC DNA was dramatically decreased in the presence of these quenchers. However, the amount remained unaltered in the presence of hydroxyl radical scavengers (KI, DMSO), superoxide scavenger (SOD, tiron) and peroxide scavenger (catalase).

### **MTT assay**

Cytotoxicity study of complex **1** and **HL** was performed on A549 (human lung adenocarcinoma cell line) and MDA-MB-231 (human epithelial breast adenocarcinoma). Beas-2B (human lung epithelial cell line) was used as non-cancerous cells. The cells were cultured in 10% FBS and DMEM (Dulbecco's Modified Eagle Medium) mixture at 37 °C and 5%  $\text{CO}_2$  atmosphere. About 8000 A549, MDA-MB-231 or Beas-2B cells were seeded in 96 well plates. After ~24 h, when the cells adhered, the complex and **HL** were added at a concentration of 0.195  $\mu$ M by diluting in 1% DMSO-DMEM medium and kept for 4 h in dark. After removing the compound containing media, DPBS (Dulbecco's phosphate-buffered saline) buffer was used for washing the cells, and one set of the cells was exposed to red light of 600-720 nm wavelength and 30 Joules  $\text{cm}^{-2}$  dose. After light treatment, DPBS was replaced with fresh DMEM media. Another set was placed in the dark with the fresh DMEM medium. Both the samples were kept for 19 h post treatment in the dark with a total incubation period of 24 h.  $\text{IC}_{50}$  values were measured from GraphPad Prism 8 software.

### **Confocal microscopy**

Around  $1 \times 10^5$  A549 cells were seeded in glass bottom petri dishes and allowed to adhere for 24 h in a  $\text{CO}_2$  incubator under aseptic conditions. After that 10  $\mu$ M of the complex was added to the glass bottom dishes and incubated at 37 °C for 4 h (with or without photoactivation). Cells were thoroughly washed with DPBS and incubated with Hoechst dye (5  $\mu$ g/ml), MitoTracker green (200 nM) and Endoplasmic Reticulum Tracker green (1 $\mu$ M) to stain the

respective organelle. Finally, the cells were washed with PBS three times and finally, images were captured using oil immersion lens with 63 X magnification. Images were captured and processed using ZEN 3.3 (blue edition software).

### **DCFDA assay**

$1 \times 10^5$  cells were seeded in glass bottom dishes and allowed to attach for 24 h in an incubator. Cells were treated with the complex (2  $\mu$ M) and incubated for 4 h in dark at 37 °C having 5% CO<sub>2</sub> environment. Cells were then washed with PBS buffer three times and stained with DCFDA (5  $\mu$ M) for 30 min at room temperature in dark. One set of plate is exposed with red light for 20 min having wavelength 600-720 nm and light dose 30 Joules cm<sup>-2</sup>. Confocal images were recorded with 10 $\times$  magnification. Images were processed by using LAS X software.

### **JC-1 assay**

Around  $1 \times 10^5$  A549 cells were plated in 12 well plates and allowed to adhere for 24 h. Cells were incubated with the complex (2  $\mu$ M) and incubated for 4 h at 37 °C in dark. Cells were then washed with PBS buffer. One set of cells was exposed to red light for 20 min and other set was kept in dark. Cells were then stained with JC-1 dye and confocal images were captured with 10 $\times$  magnification. Images were captured and processed in ZEN 3.3 (blue edition) software.

### **Annexin V-FITC/Propidium Iodide assay**

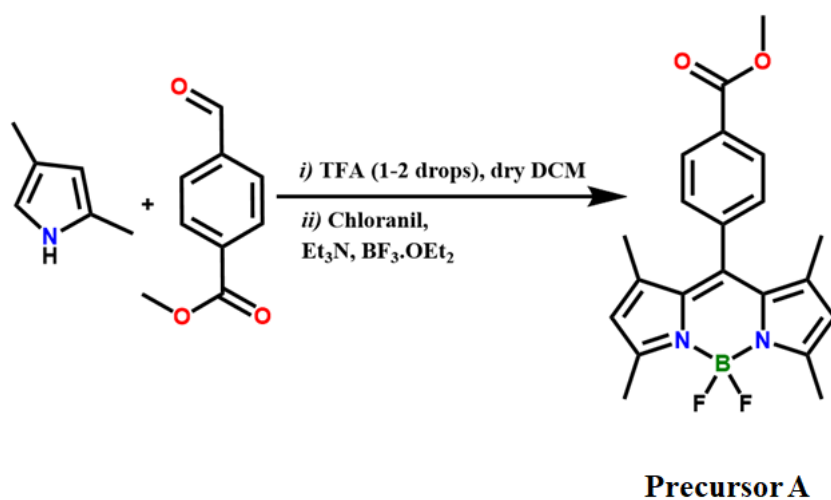
Approximately  $10^5$  cells were plated in 6 well plates and incubated for 24 h before addition of complex 1. Cells were then treated with the complex at 1  $\mu$ M concentration and kept for 4 h incubation in dark. Then, one set of the cells was exposed to red light for 20 min (600-720 nm wavelength and 30 Joules cm<sup>-2</sup>) and the other set was kept in the dark. Cells were kept further 1 h post incubation. Cells were then trypsinized and single cell suspension was prepared. After that 500  $\mu$ l binding buffer was added to each sample. After that 1  $\mu$ M annexin and 1  $\mu$ M propidium iodide were added to each sample containing binding buffer and kept for 10 min incubation. Finally, flow cytometry analysis was performed.

### **$\beta$ -Tubulin immunostaining assay**

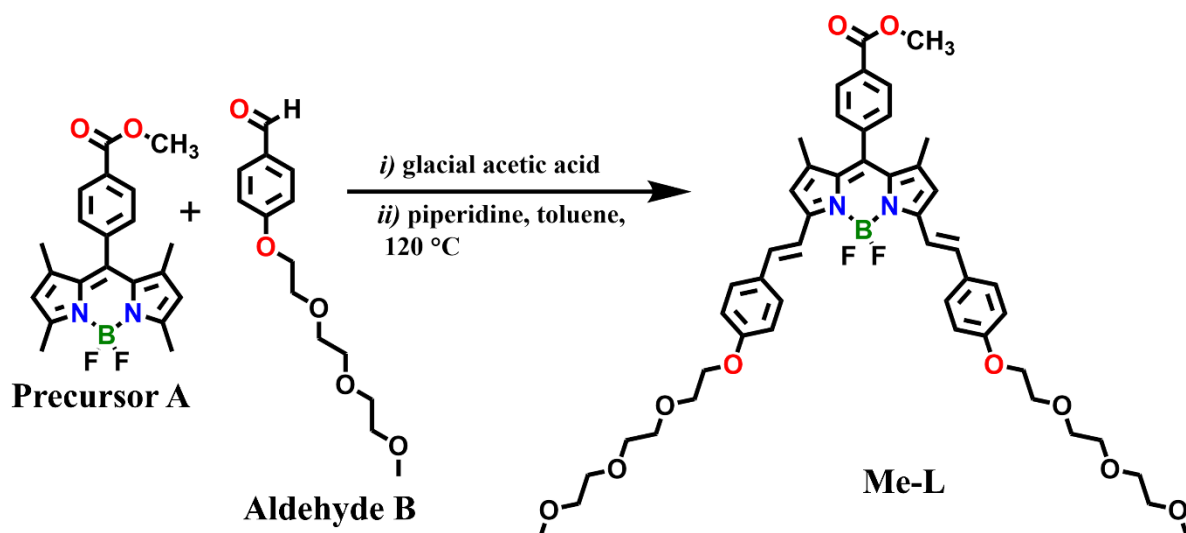
A total of around  $10^5$  cells were seeded onto coverslips in a 12-well plate and left to adhere for 12 h. The cells were then treated with the complex and incubated at 37°C in the dark for a period of 4 h. After photoirradiation and subsequent washes with PBS, the samples were fixed



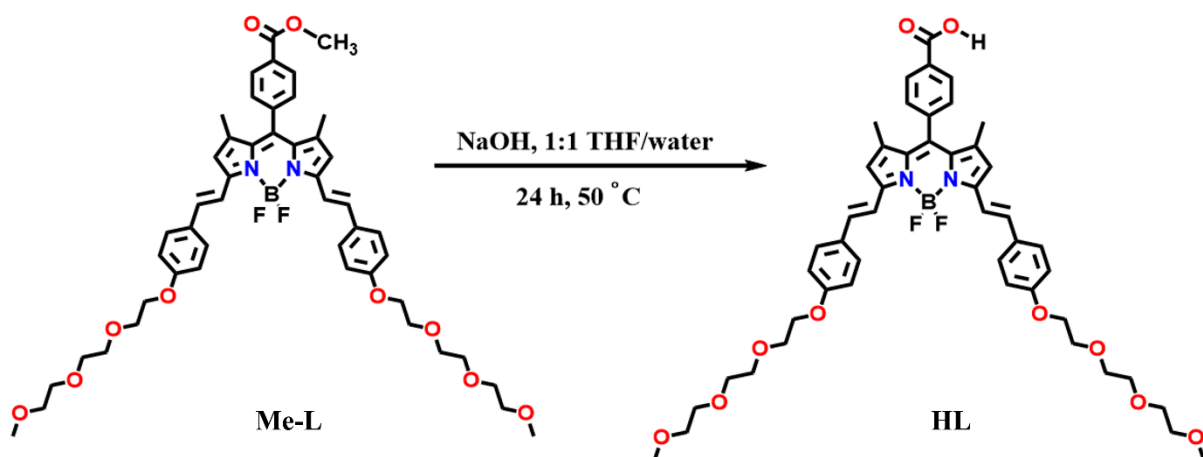
with a 4% paraformaldehyde (PFA) solution for 15 min. Following another set of PBS washes, the cells were permeabilized using a solution of 1% Triton in FBS for 15 min. After three washes, the cells were subjected to blocking with a solution of 0.3% Triton in 10% FBS for a duration of 1.5 h. Subsequently, the cells were incubated with a beta-tubulin antibody at a dilution of 1:500 for 1 h at room temperature, followed by further washes with PBS. To perform the secondary staining for immunofluorescence, the cells were subjected to a 1 h incubation at room temperature with Anti-Rabbit Alexa 488 (diluted at 1:500). Following the incubation, the cells were carefully washed with PBS. For nuclear staining, DAPI was applied at a concentration of 30 nM. Coverslips were mounted with DABCO and securely sealed to preserve the prepared samples. The subsequent visualization of the samples was carried out using Olympus 1X 83 epifluorescence microscope.



**Scheme S1.** Scheme for the synthesis of precursor A. TFA is trifluoroacetic acid and DCM is dichloromethane.



**Scheme S2.** Scheme for the synthesis of Me-L.



**Scheme S3.** Scheme for the synthesis of HL. THF is tetrahydrofuran.

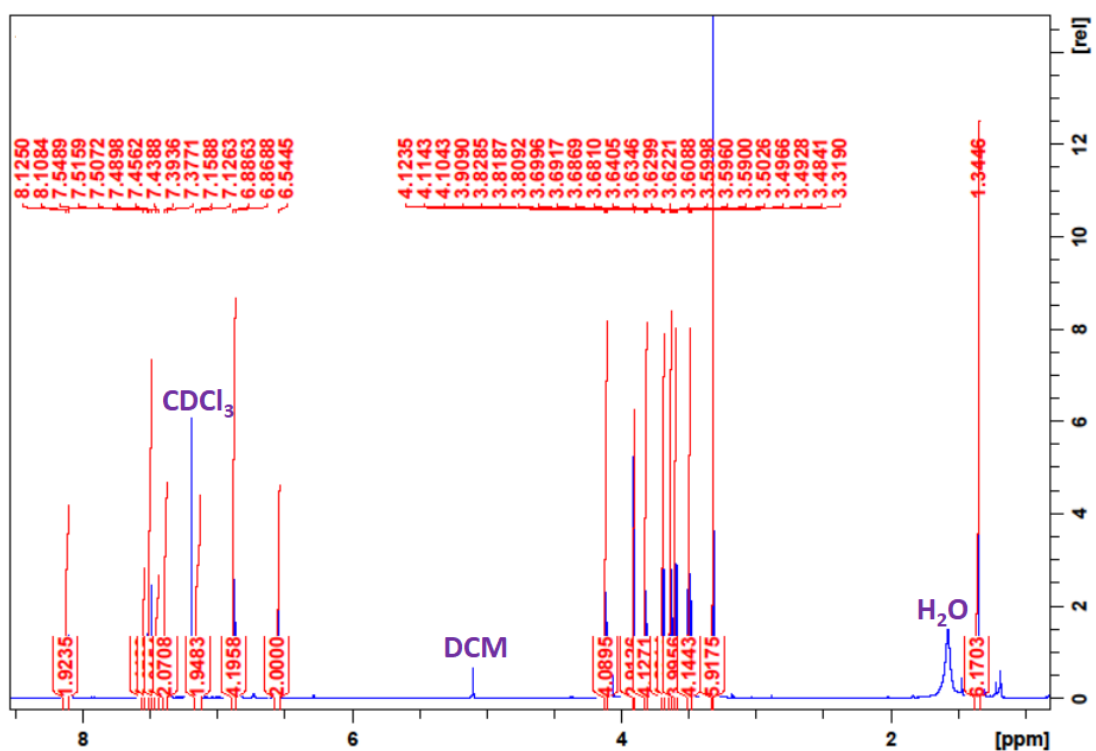


Fig. S1. <sup>1</sup>H NMR spectrum of ligand precursor Me-L in CDCl<sub>3</sub>.

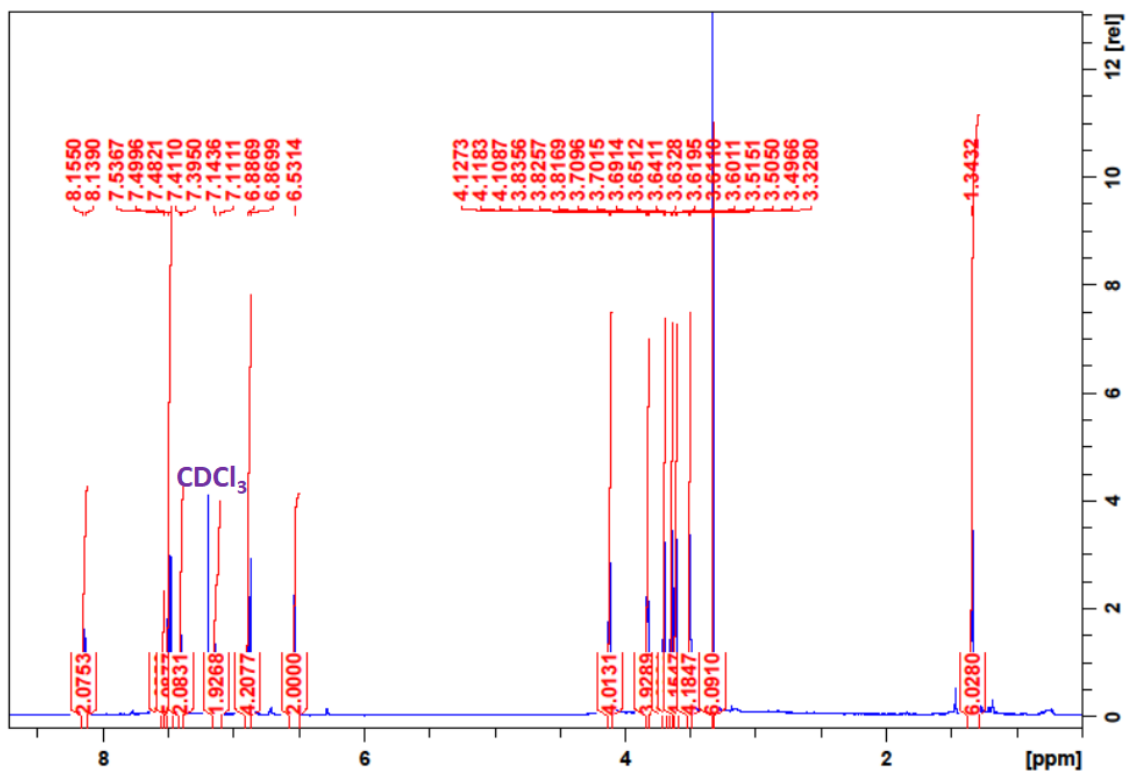


Fig. S2. <sup>1</sup>H NMR spectrum of ligand HL in CDCl<sub>3</sub>.

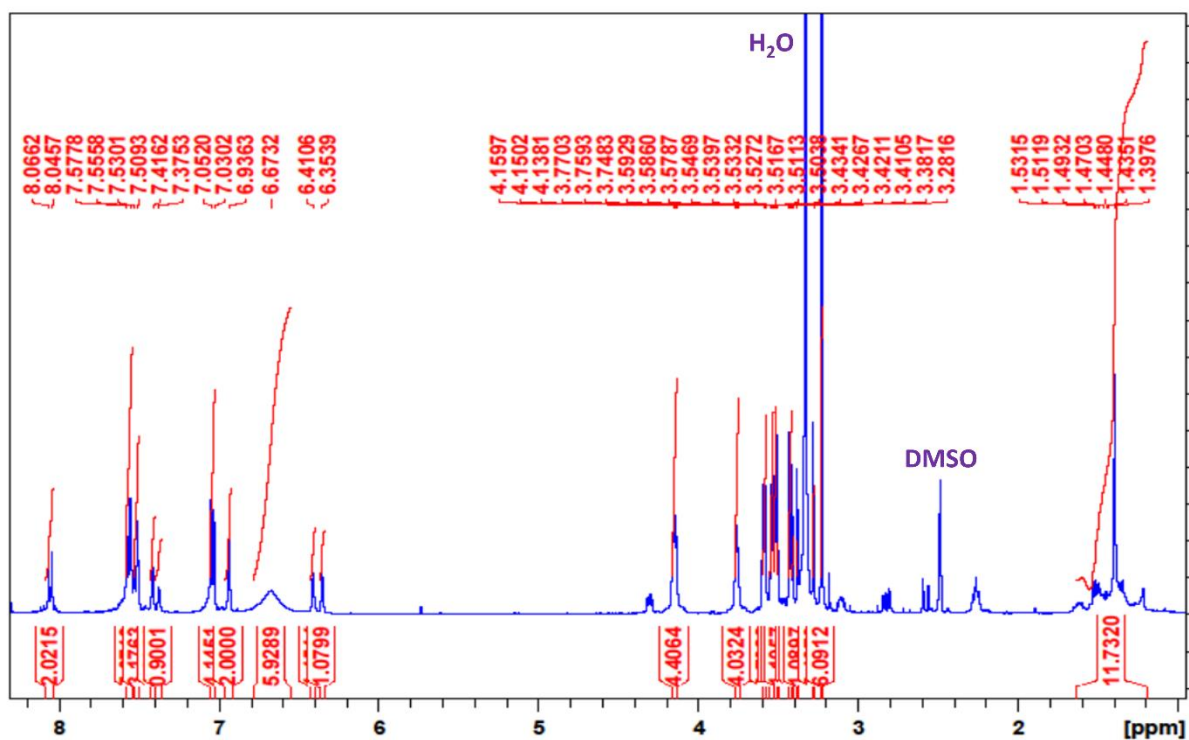


Fig. S3.  $^1\text{H}$  NMR spectrum of complex **1** in  $\text{DMSO-d}_6$ . The metal-bound ammine 6H peaks appeared broad.

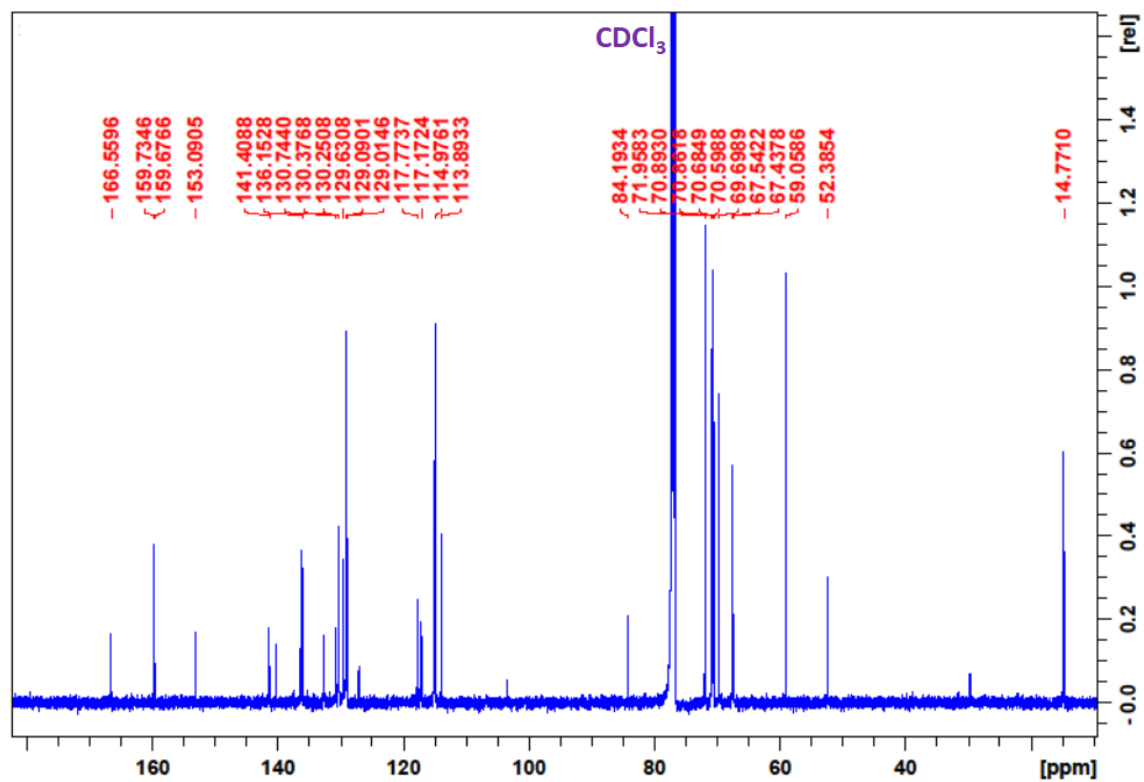


Fig. S4.  $^{13}\text{C}$  NMR spectrum of Me-L in  $\text{CDCl}_3$ .

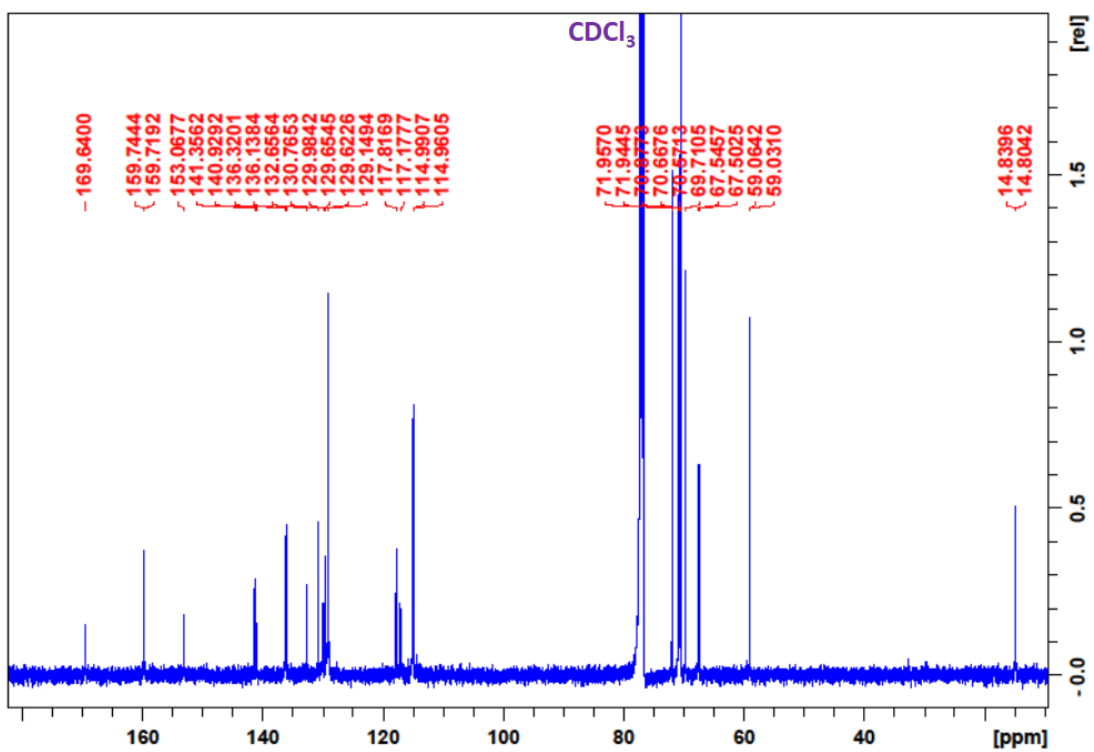


Fig. S5.  $^{13}\text{C}$  NMR spectrum of HL in  $\text{CDCl}_3$ .

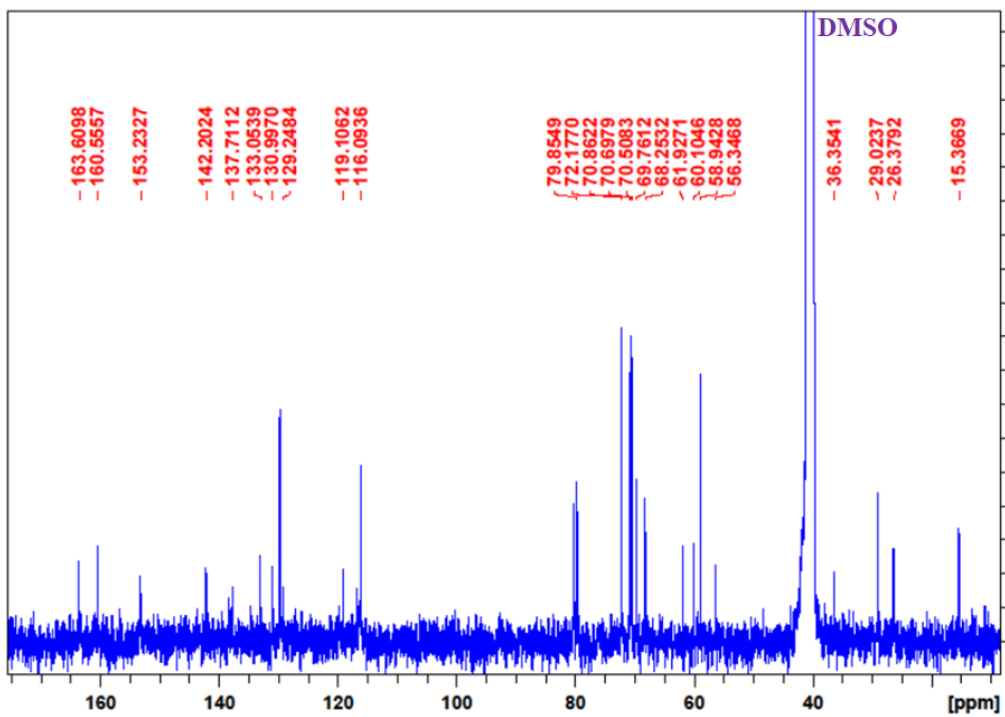


Fig. S6.  $^{13}\text{C}$  NMR spectrum of complex 1 in  $\text{DMSO-d}_6$ .

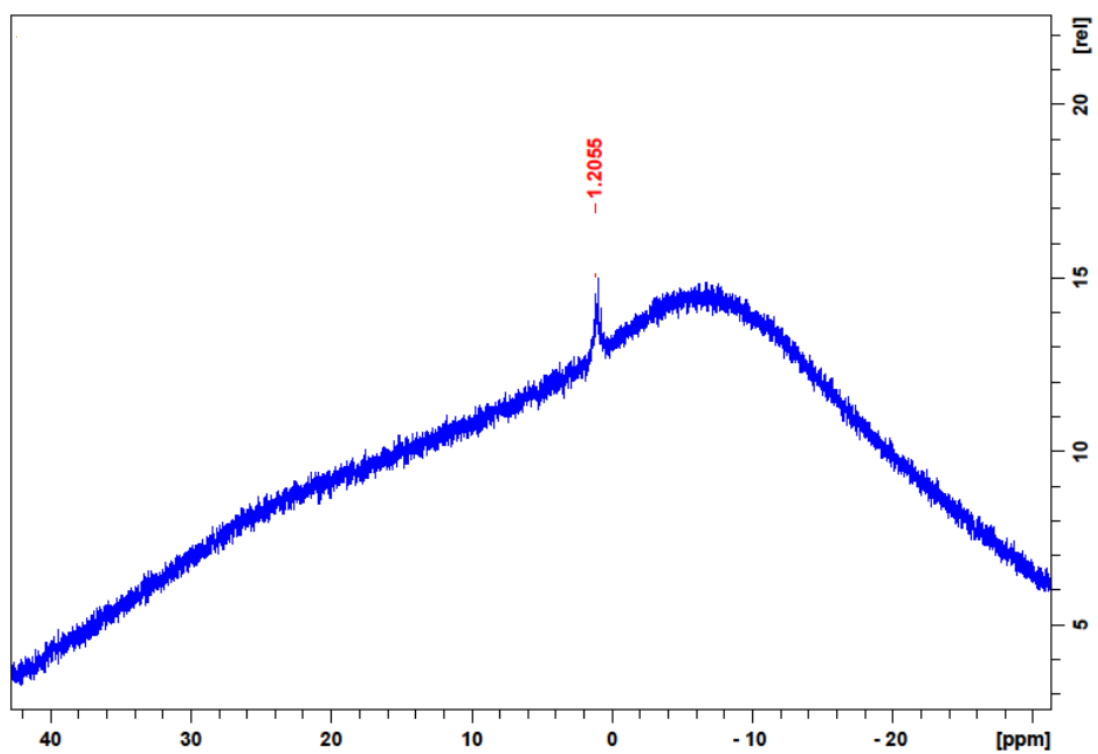


Fig. S7.  $^{11}\text{B}$  NMR spectrum of Me-L in  $\text{CDCl}_3$ .

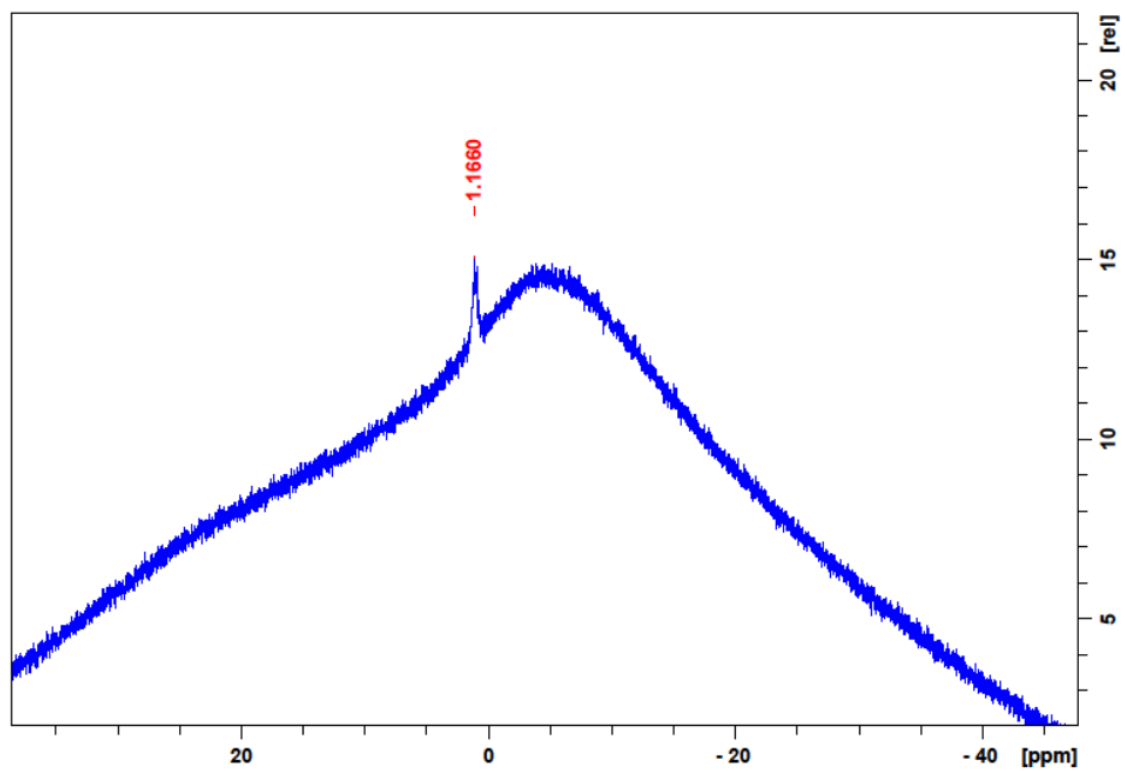
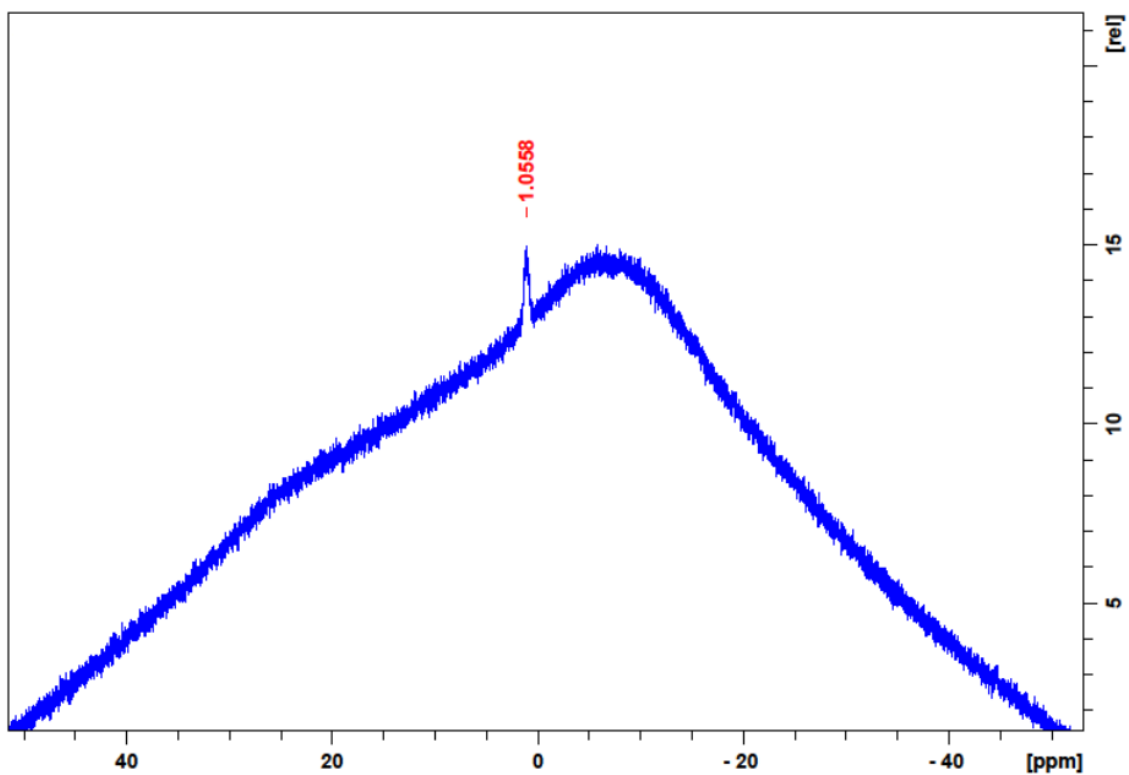
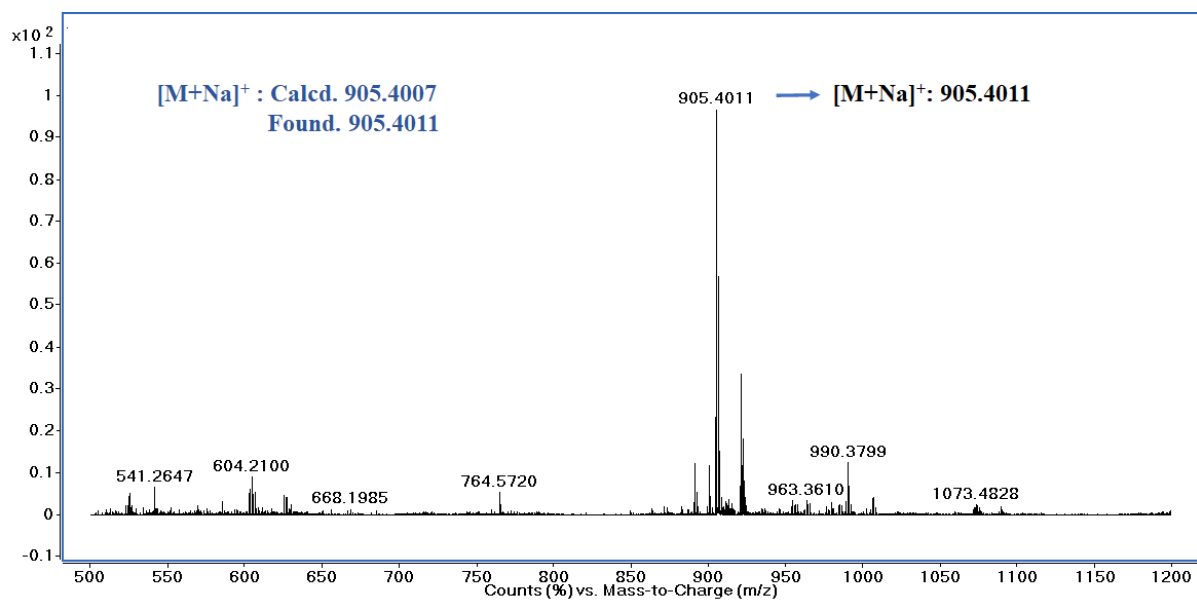


Fig. S8.  $^{11}\text{B}$  NMR spectrum of HL in  $\text{CDCl}_3$ .



**Fig. S9.**  $^{11}\text{B}$  NMR spectrum of complex **1** in  $\text{DMSO-d}_6$ .



**Fig. S10.** Mass spectrum of Me-L recorded in acetonitrile with a peak corresponding to  $[\text{M}+\text{Na}]^+$  ( $m/z$ ) at 905.4011.

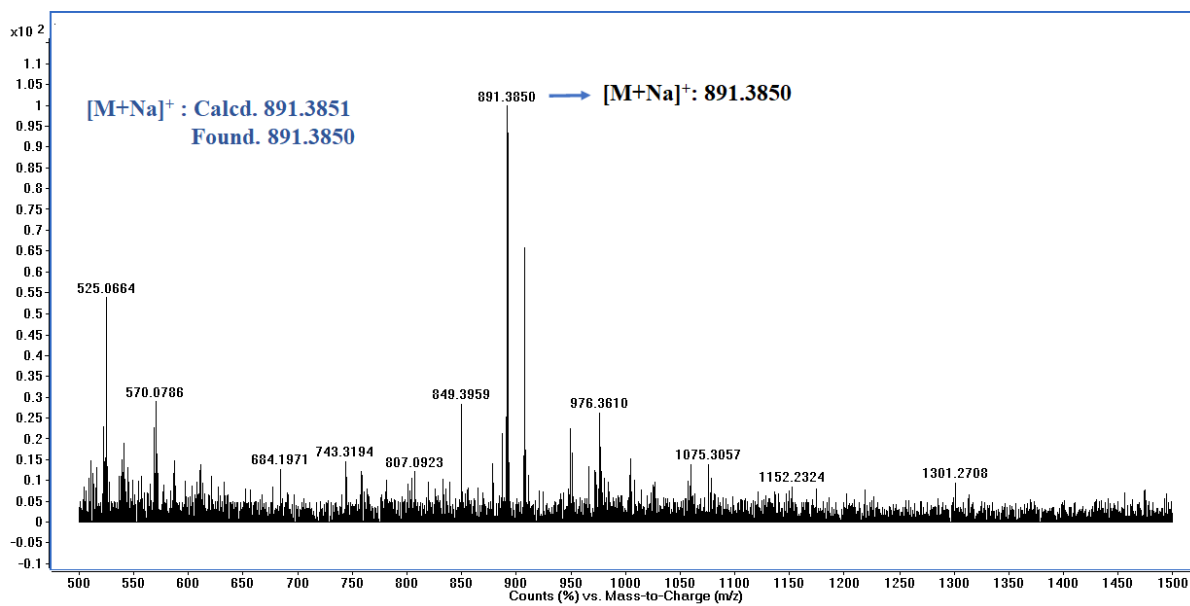


**Fig. S11.** Mass spectrum of HL recorded in acetonitrile with a peak corresponding to  $[M+Na]^+$  ( $m/z$ ) at 891.3850.



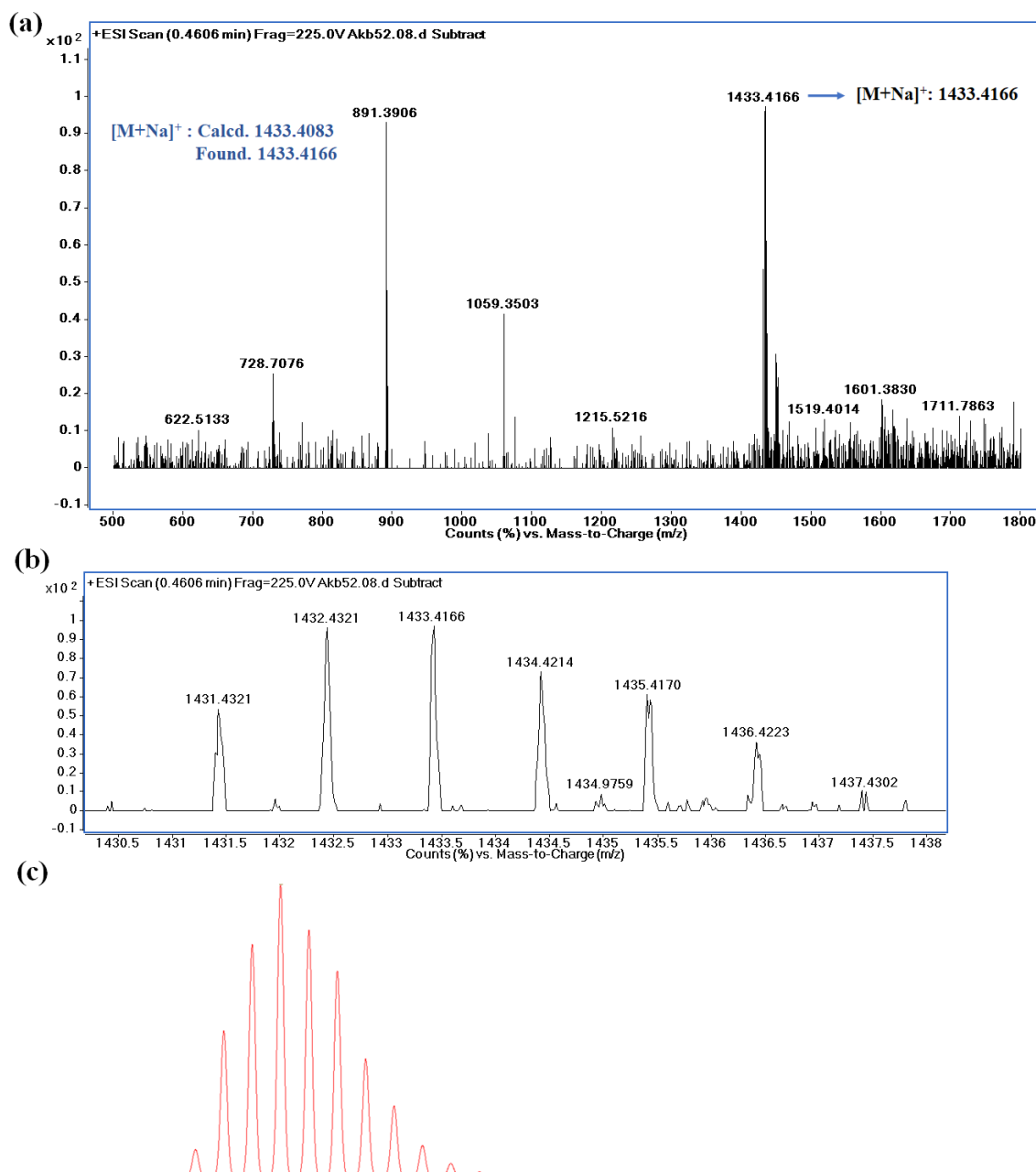


**Fig. S12.** (a) Mass spectrum of complex **1** recorded in acetonitrile with a peak corresponding to  $[M+Na]^+$  ( $m/z$ ) at 1433.4166. (b) Isotopic distribution of the complex showing the presence of platinum. (c) Simulated isotopic distribution pattern.

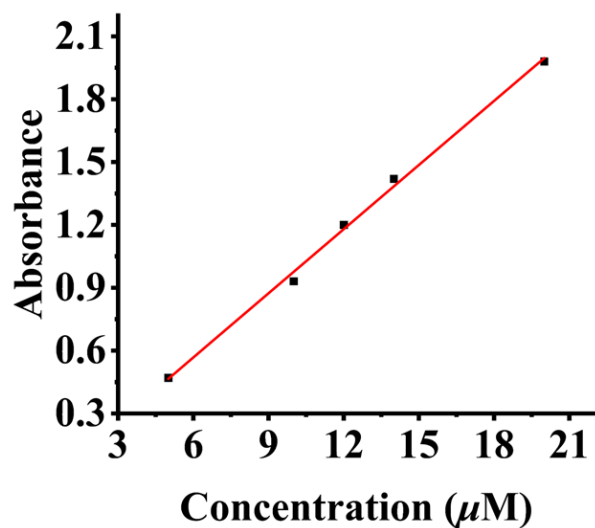


**Fig. S13.** UV-visible spectral absorbance of complex 1 recorded at different concentration in DMSO. The absorbance was plotted against concentration.

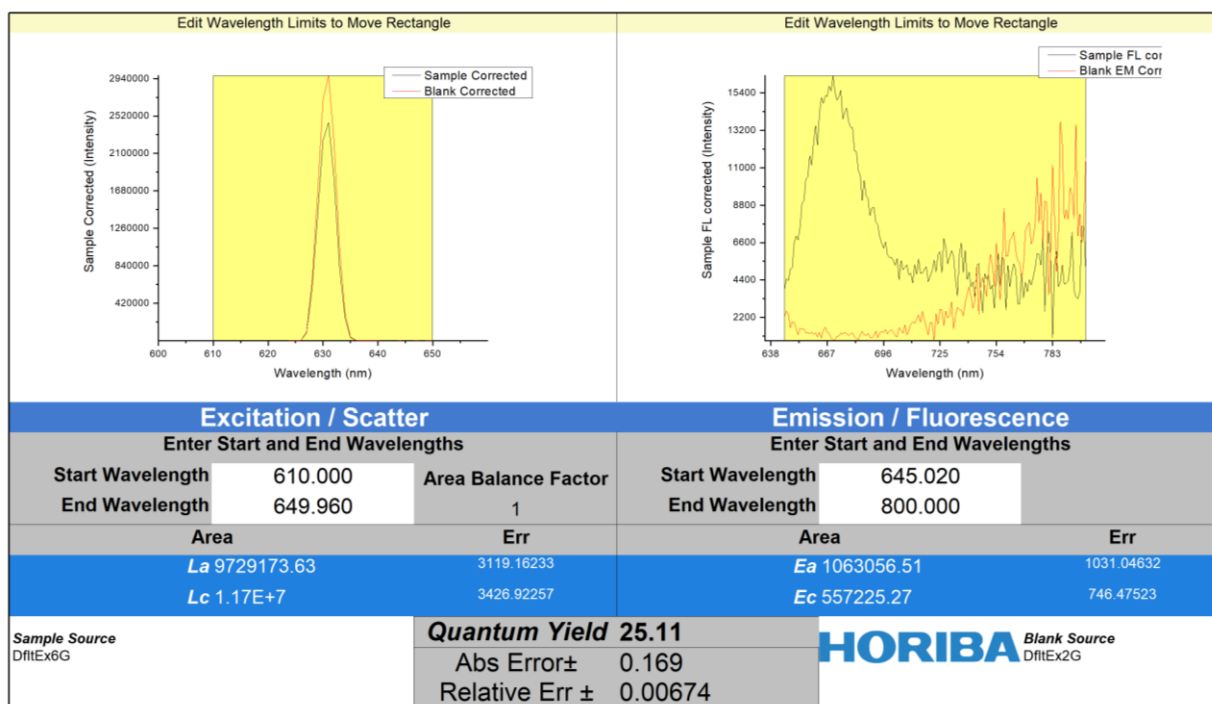


**Fig. S14.** Fluorescence quantum yield for ligand HL in DMSO.

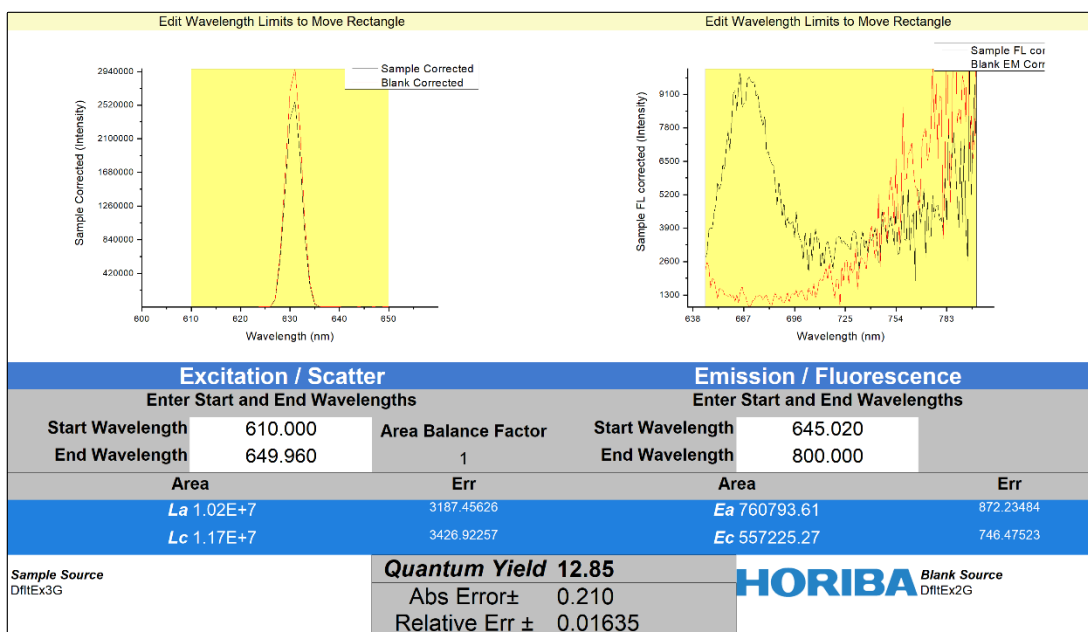


Fig. S15. Fluorescence quantum yield for complex **1** in DMSO.

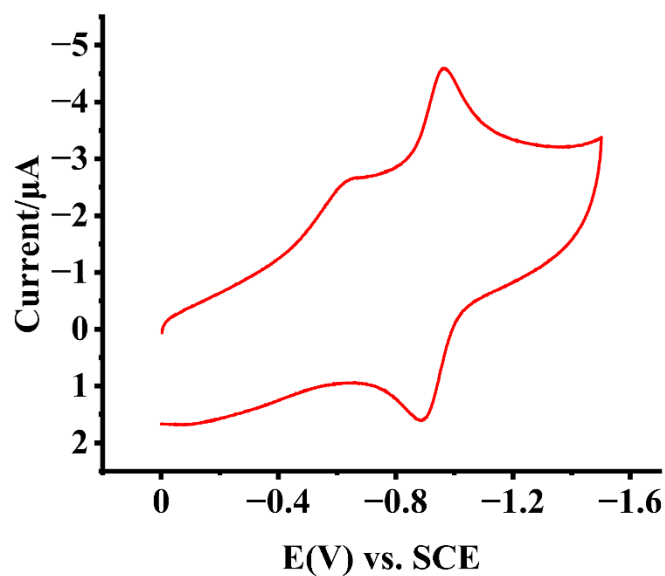
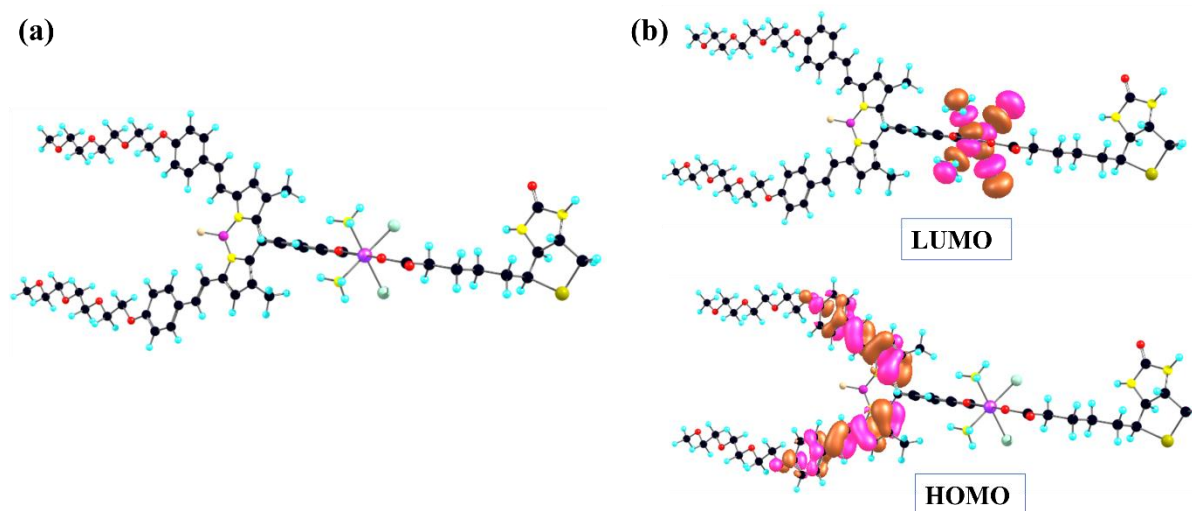
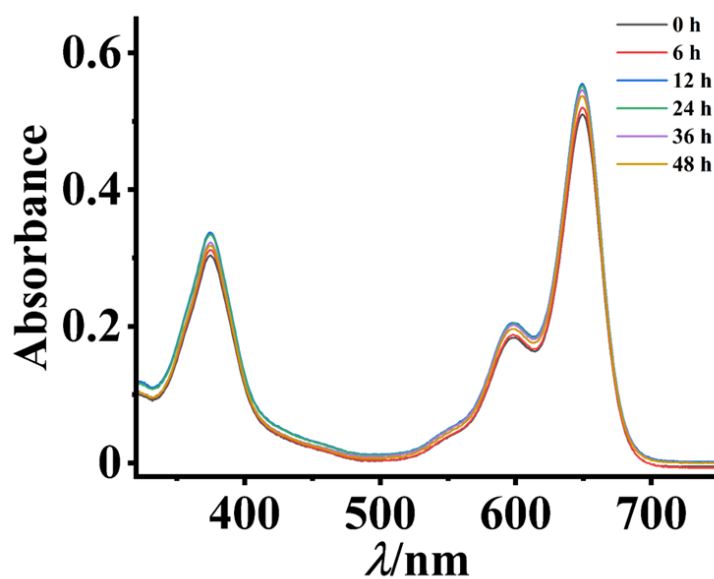


Fig. S16. Cyclic voltammogram of complex **1** in 10% aq. DMF at a scan rate of 100 mV s<sup>-1</sup>.



**Fig. S17.** (a) Optimized geometry of the *cis,cis,trans*-Pt(IV) complex **1** as obtained from the quantum calculations using B3LYP/LanL2DZ level of theory. The six-coordinate geometry has a cisplatin basal plane and two axial ligands having biotin and a BODIPY moiety. (b) Nodal patterns of HOMO and LUMO as generated from the optimized structure.



**Fig. S18.** Time-dependent stability studies of complex **1** in 1:1 (v/v) DMSO/DPBS (pH =7.4) under dark condition. It shows no major spectral changes over time and the spectral features remained essentially the same.

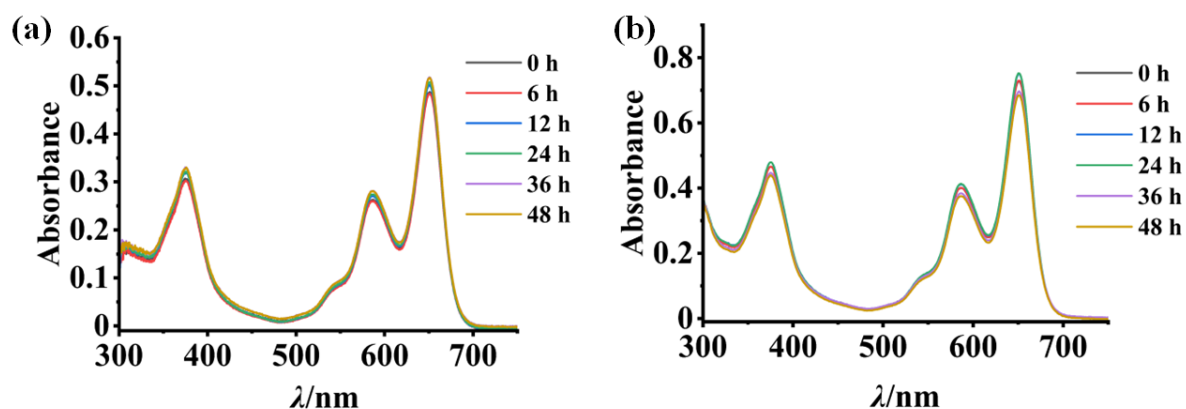


**Fig. S19.** Time-dependent stability studies of complex **1** in 1:1 (v/v) DMSO/DPBS under dark condition at different pH condition: (a) pH = 3.0 and (b) pH = 9.0.

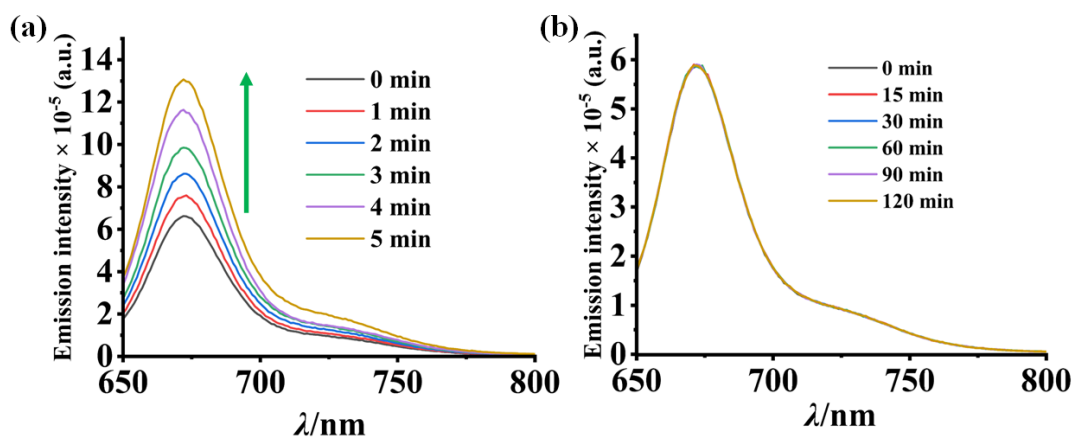


**Fig. S20.** (a) An increase in emission intensity of Pt(IV) complex **1** in 1:1 (v/v) DMSO/DPBS ( $\lambda_{\text{ex}} = 630$  nm, pH=7.4) upon red light (642 nm laser) irradiation suggesting possible release of the emissive BODIPY ligand. The traces were taken up to 5 min. (b) Emission intensity of the complex remained unaltered under dark conditions indicating its high dark stability. Data were recorded up to 120 min in the dark.

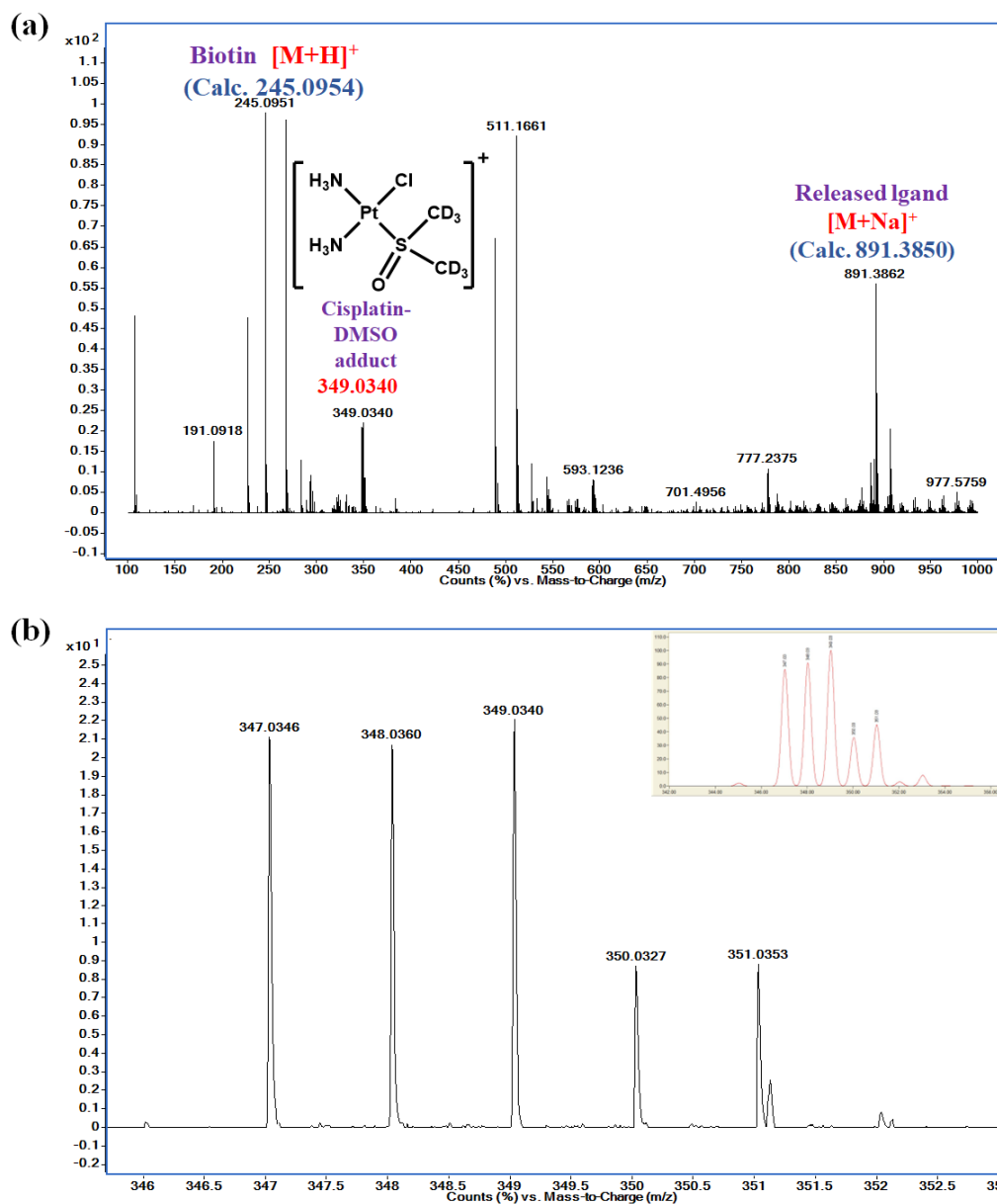


**Fig. S21.** (a) ESI-MS of light-exposed complex **1** solution (used for NMR study). The 349.0340 peak is assignable to species formulated as  $[\text{Pt}(\text{NH}_3)_2\text{Cl}(\text{DMSO-d}_6)]^+$ , 245.0951 and 891.3850 peaks are due to free biotin and BODIPY ligand respectively released from the complex after light irradiation. (b) Isotopic distribution of  $[\text{Pt}(\text{NH}_3)_2\text{Cl}(\text{DMSO-d}_6)]^+$  adduct with the inset showing the simulated isotopic distribution indicating the presence of platinum.

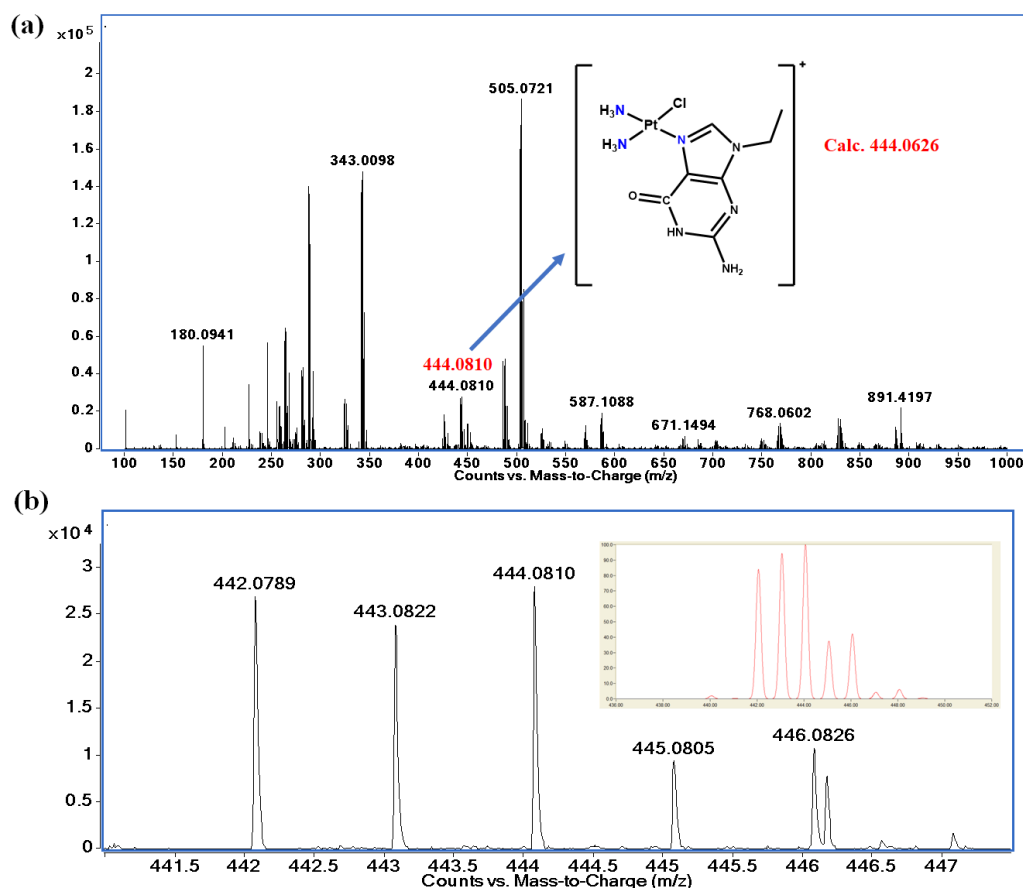


**Fig. S22.** (a) ESI-MS study of DNA binding ability of light exposed solution with model nucleobase 9-ethylguanine (9-EtG). Experiment was performed by taking light exposed sample with 4 equiv. 9-EtG after 6 h of incubation. The peak corresponding to 444.0810 m/z suggests the formation of the species  $[\text{Pt}(\text{NH}_3)_2\text{Cl}(9\text{-EtG})]^+$ . (b) Isotopic distribution pattern of  $[\text{Pt}(\text{NH}_3)_2\text{Cl}(9\text{-EtG})]^+$  and the inset shows the simulated isotopic distribution pattern indicating the presence of platinum and overall one charge of the complex.

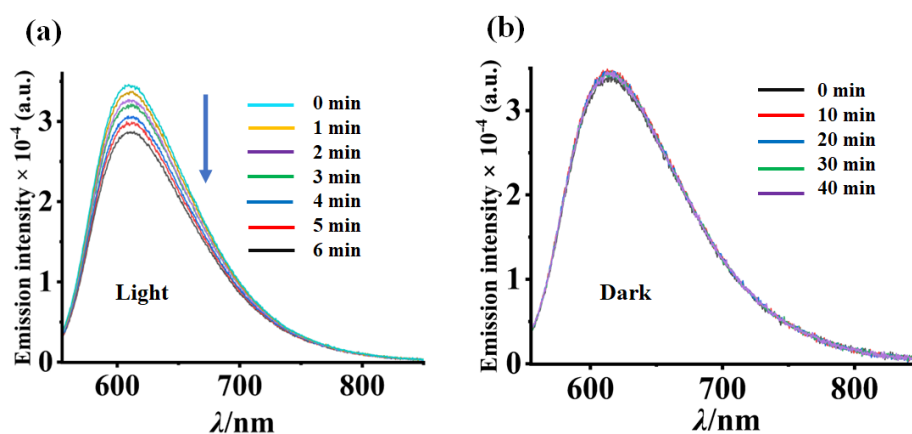


**Fig. S23.** (a) Ethidium bromide (EB) assay showing a decrease in the emission intensity indicating DNA crosslink formation upon light irradiation. A decrease in the emission intensity of EB (50  $\mu\text{M}$ ) at 605 nm was observed when the ct-DNA and complex **1** (30  $\mu\text{M}$ ) containing solution was photo irradiated. (b) Emission intensity of EB remained the same in dark for over 40 min period.

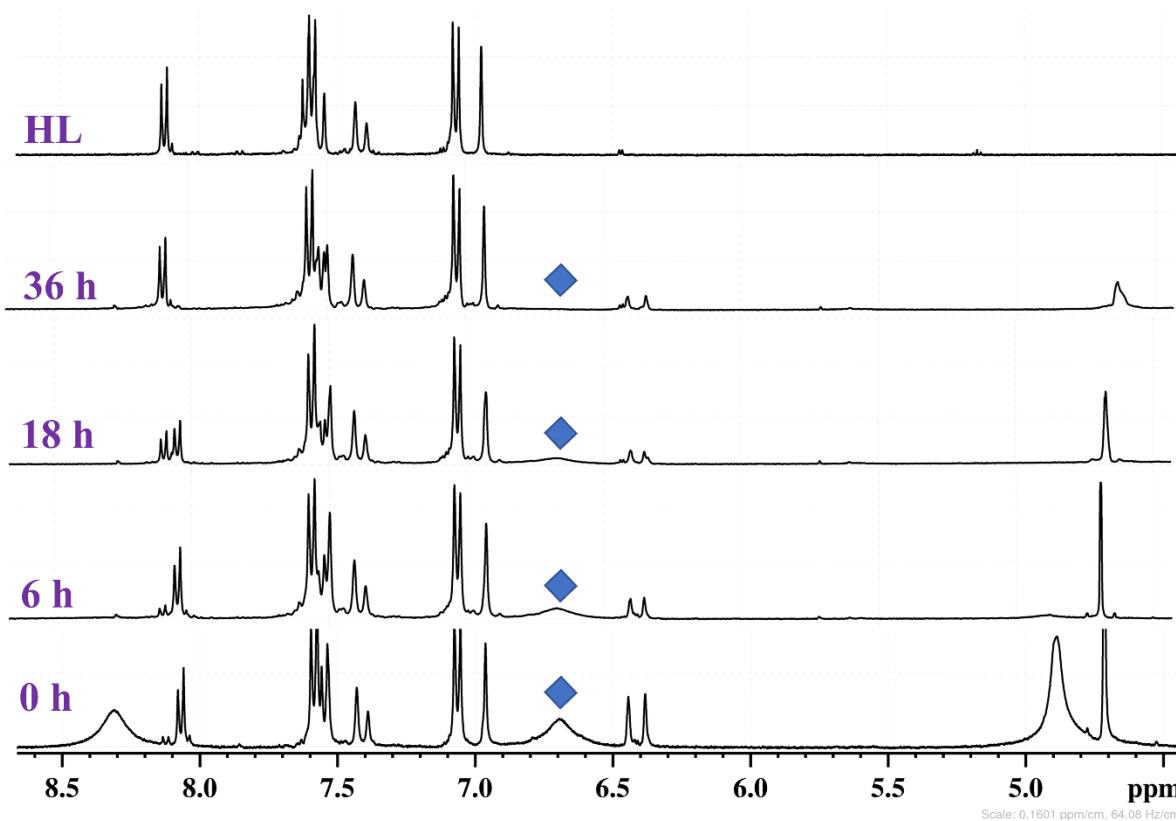


**Fig. S24.** Time-dependent <sup>1</sup>H NMR spectra of complex **1** in presence of 10 equiv. ascorbic acid as a reducing agent. The signal for six ammine protons (marked with blue diamond motif) disappeared on metal reduction from Pt(IV) to Pt(II) in presence of ascorbic acid as a reducing agent thus releasing the ligand HL and biotin. Broad peaks near 8.3 ppm and 4.4 ppm are due to ascorbic acid.

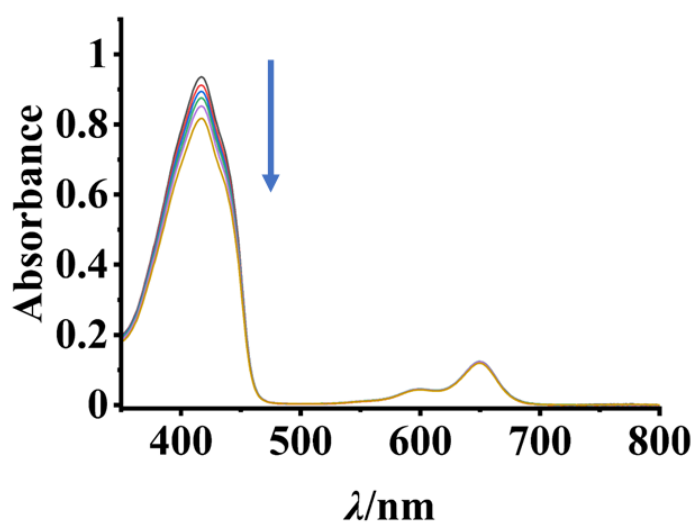


**Fig. S25.** Changes in the absorption spectra of the solution having DBBF (1,3-diphenylisobenzofuran) and ligand HL in 50:1 molar concentration ratio on red light exposure (642 nm, 100 mW) in DMSO.



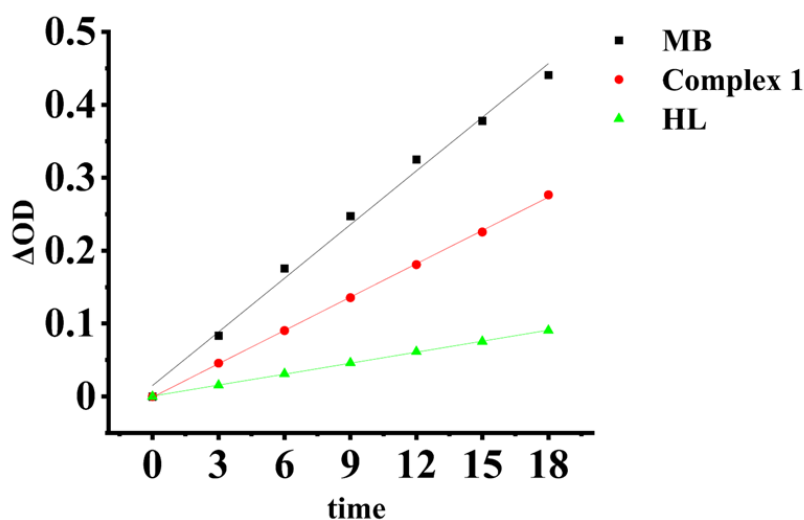


**Fig. S26.**  $\Delta$ OD vs. irradiation time for determining singlet oxygen quantum yield ( $\Phi_{\Delta}$ ) of complex **1** and HL (MB, methylene blue used as a control). The plot shows the importance of platinum for the high  $\Phi_{\Delta}$  value of complex **1** compared to the ligand HL alone.

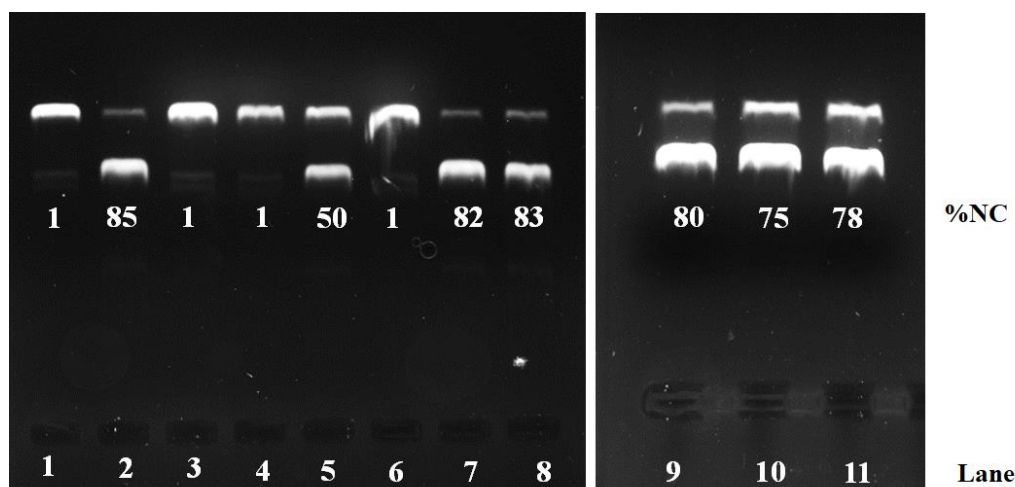


**Fig. S27.** (a) Gel diagram showing photocleavage of pUC19 DNA (33  $\mu$ M) in presence of complex **1** (30  $\mu$ M) upon 642 nm red laser irradiation for 45 min duration. Lanes are: (1) DNA control (in light) showing SC form only, (2) DNA + complex **1** (in light) showing essential formation of NC form from SC form, (3) DNA + complex **1** (in dark) showing SC form. Lanes (4-11) are showing mechanistic aspects of the photocleavage of pUC19 DNA in presence of complex **1** and different scavengers/quenchers/additives, namely, KI, 6  $\mu$ M; TEMP, 6  $\mu$ M; NaN<sub>3</sub>, 6  $\mu$ M; DHN, 6  $\mu$ M; DMSO, 4  $\mu$ L; SOD, 4 units; catalase, 4 units; Tiron, 6  $\mu$ M using red laser light (642 nm) irradiation. Lanes are: (4) DNA + complex **1** + NaN<sub>3</sub> (showing quenching), (5) DNA + complex **1** + TEMP (showing partial quenching), (6) DNA + complex **1** + DHN (1,5-dihydroxynapthalene) (showing quenching), (7) DNA + complex **1** + KI, (8) DNA + complex **1** + DMSO, (9) DNA + complex **1** + catalase, (10) DNA + complex **1** + Tiron, and (11) DNA + complex **1** + SOD. Lanes 7-11 show no apparent scavenging effect of the reagents added giving %NC within 75-83% which is similar to 85% of NC DNA formed (lane 2).

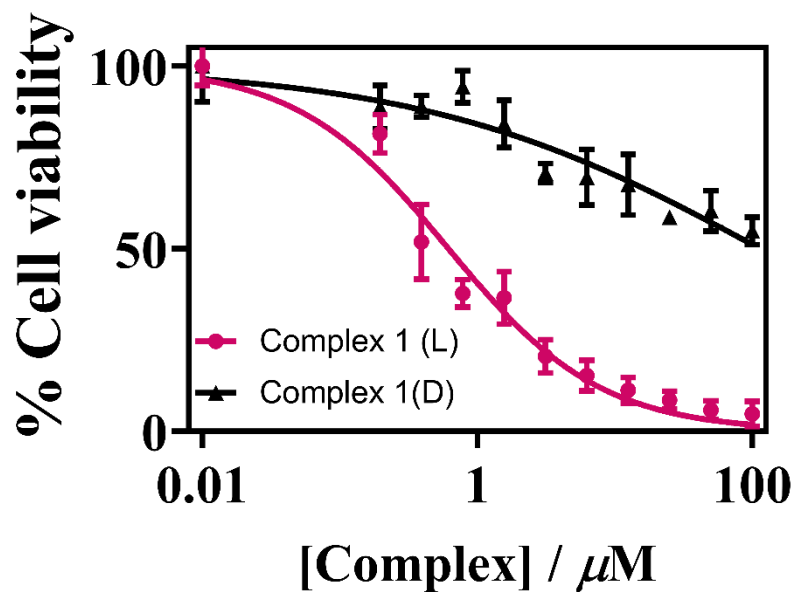


**Fig. S28.** Cell viability plots obtained from MTT assay of complex 1 in A549 cells on light exposure (L, 600-720 nm, 20 min exposure, light dose: 30 Joules  $\text{cm}^{-2}$ ) and in dark (D) condition.

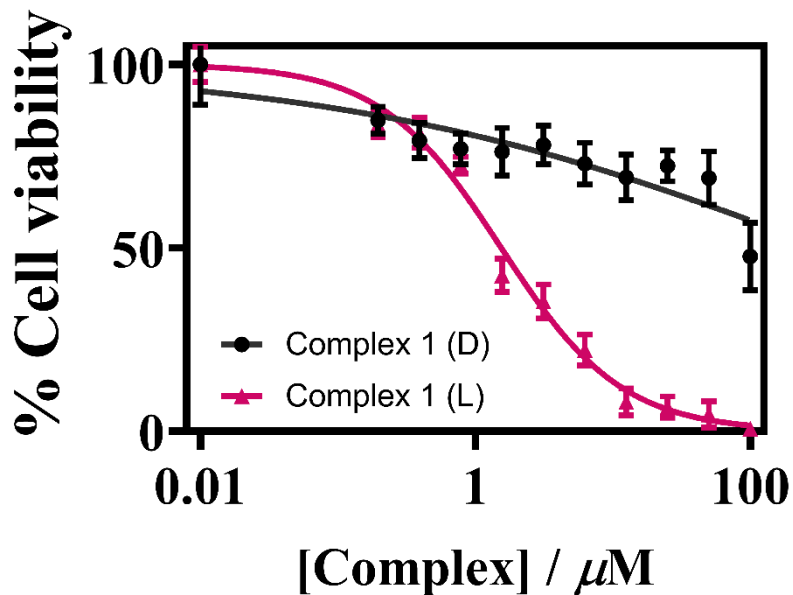


**Fig. S29.** Cell viability plots obtained from MTT assay of complex 1 in MDA-MB-231 cells on light exposure (L, 600-720 nm, 20 min exposure, light dose: 30 Joules  $\text{cm}^{-2}$ ) and in dark (D) condition.

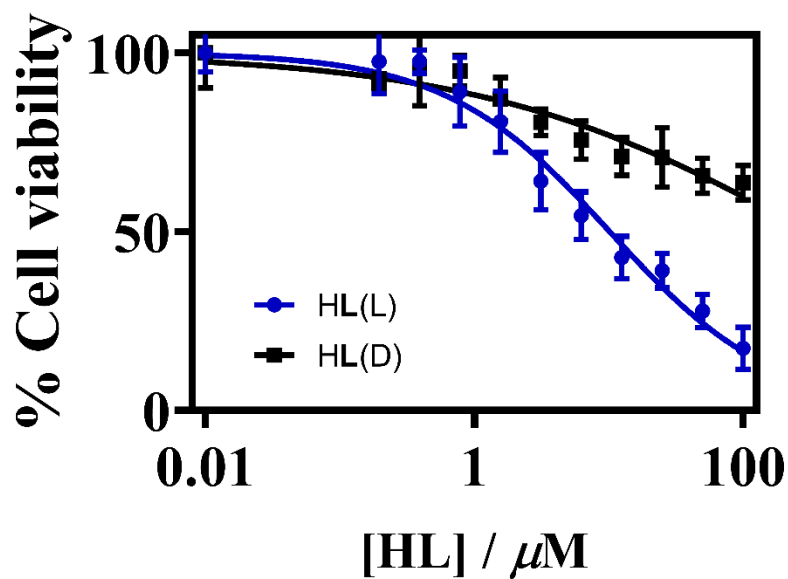


**Fig. S30.** Cell viability plots obtained from MTT assay of ligand HL in A549 cells on light exposure (L, 600-720 nm, 20 min exposure, light dose: 30 Joules  $\text{cm}^{-2}$ ) and in dark (D) condition.

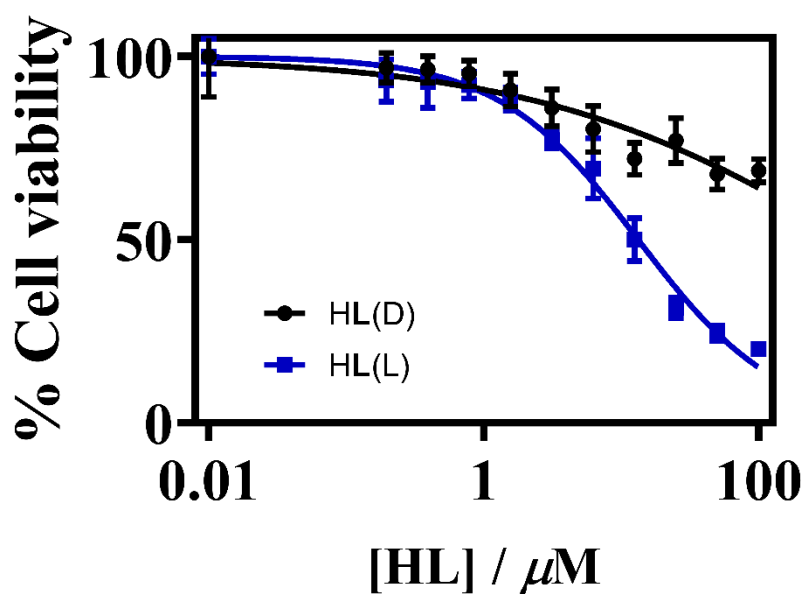


**Fig. S31.** Cell viability plots obtained from MTT assay of ligand HL in MDA-MB-231 cells on light exposure (L, 600-720 nm, 20 min exposure, light dose: 30 Joules  $\text{cm}^{-2}$ ) and in dark (D) condition.

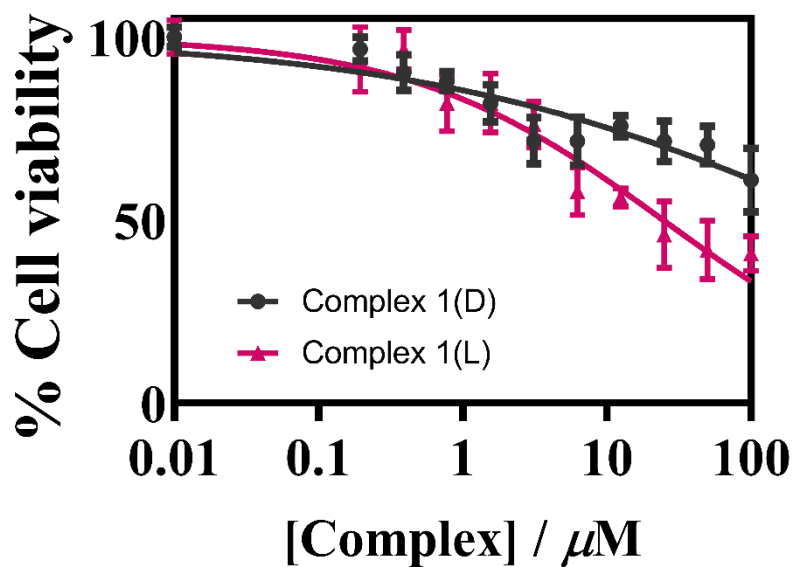


**Fig. S32.** Cell viability plots obtained from MTT assay of complex **1** in Beas-2B cells on light exposure (L, 600-720 nm, 20 min exposure, light dose: 30 Joules  $\text{cm}^{-2}$ ) and in dark (D) condition.

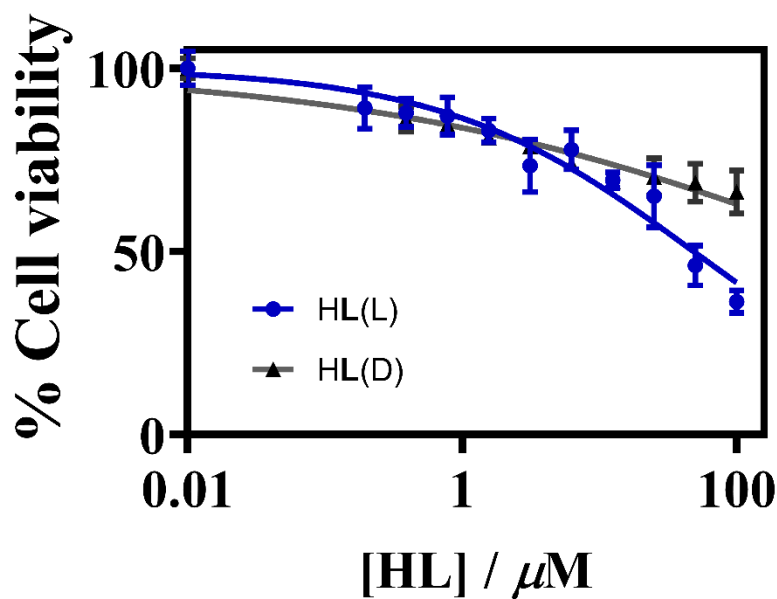


**Fig. S33.** Cell viability plots obtained from MTT assay of ligand **HL** in Beas-2B cells on light exposure (L, 600-720 nm, 20 min exposure, light dose: 30 Joules  $\text{cm}^{-2}$ ) and in dark (D) condition.

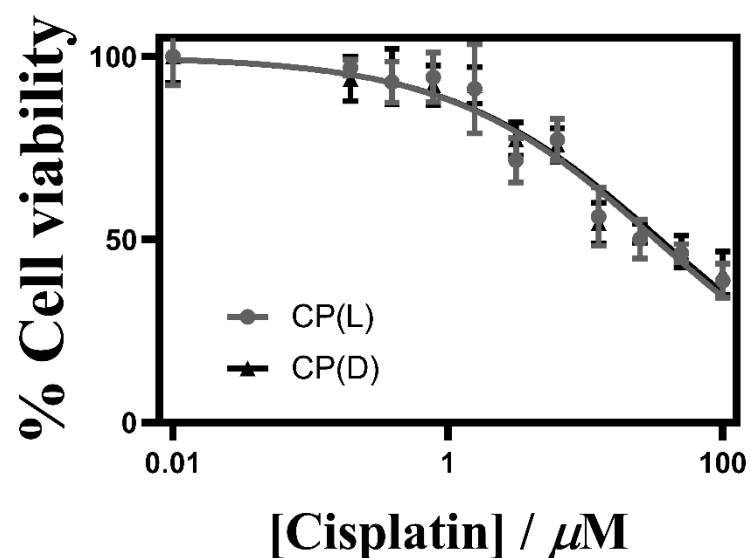


**Fig. S34.** Cell viability plots obtained from MTT assay of cisplatin in A549 cells on light exposure (L, 600-720 nm, 20 min exposure, light dose:  $30 \text{ Joules cm}^{-2}$ ) and in dark (D) condition.

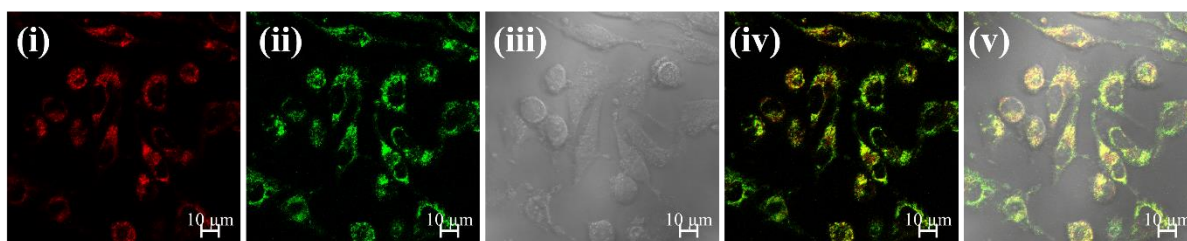


**Fig. S35.** Confocal images of A549 cells incubated with complex **1**. The panels are: (i) complex **1**-based emission, (ii) green emitting ER tracker (ERG), (iii) bright field, (iv) merged image without bright field and (v) merged image with bright field. Scale bar  $20 \mu\text{m}$ .

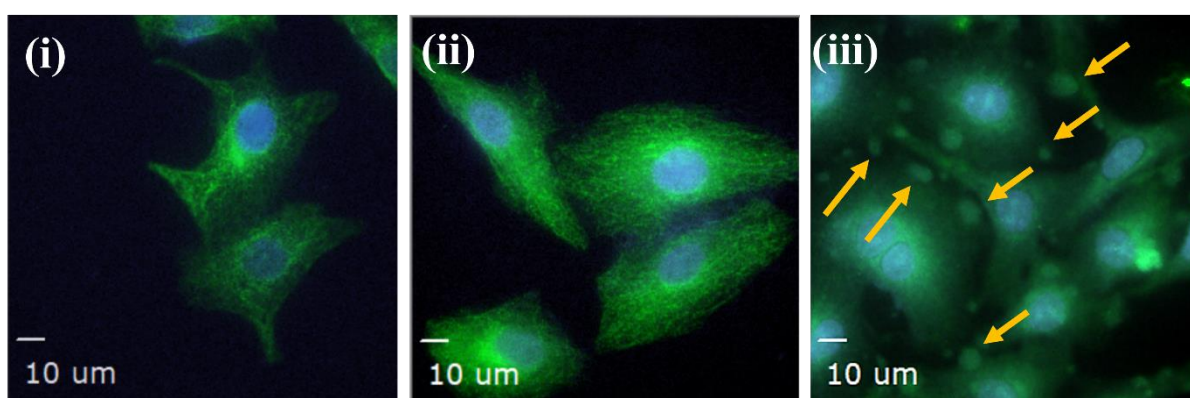


**Fig. S36.** Immunofluorescence study to investigate the impact of light treatments on the microtubule network of the complex treated A549 cells. Microtubules were visualized with  $\beta$ -tubulin antibody interacting with a secondary antibody tagged with Alexa Fluor 488. Panels are: (i) untreated cells, (ii) dark set, and (iii) light set. Apoptotic bodies are marked with yellow arrows in panel (iii).

**Table S1.** Coordinates of optimized geometry for complex **1** obtained from DFT using B3LYP/LanL2DZ level of theory for all atoms

---

Pt	8.8690950000	0.5668980000	-1.5784380000
N	8.4855450000	-0.9088540000	-3.0266500000
H	8.7217850000	-1.7855800000	-2.5417200000
N	8.3238340000	2.2128180000	-2.7700830000
H	7.3544720000	2.1381780000	-3.0883340000
H	8.4379860000	3.0162280000	-2.1370650000
Cl	9.5462830000	-1.3349550000	-0.2457470000
Cl	9.3746590000	2.2866170000	0.0464400000
H	9.1321990000	-0.7425970000	-3.8054560000
O	10.6070700000	0.7635250000	-2.6538420000
O	6.8641250000	0.4176010000	-1.1514560000
C	6.2929020000	0.3118290000	0.0923620000
O	6.9155810000	0.2686970000	1.1640810000
C	4.0713660000	0.2934290000	-1.1868910000
C	4.0792610000	0.1716090000	1.2456060000
C	2.6672370000	0.2475880000	-1.1822590000
H	4.6146260000	0.3580330000	-2.1239020000
C	2.6766050000	0.1273770000	1.2472550000
H	4.6442030000	0.1429390000	2.1726570000
C	1.9556840000	0.1665140000	0.0341280000
H	2.1176990000	0.2766120000	-2.1197920000
H	2.1372150000	0.0636420000	2.1887120000
C	0.4567200000	0.1271830000	0.0323460000
C	-0.2130620000	-1.1149640000	-0.0215840000
C	-0.2743690000	1.3350020000	0.0811130000
N	-1.6243820000	-1.1683970000	-0.0384090000
C	0.2765260000	-2.4780870000	-0.0533590000

N	-1.6866240000	1.3199980000	0.0650500000
C	0.1471510000	2.7183190000	0.1640530000
C	-2.0237940000	-2.4860460000	-0.0780200000
B	-2.5453620000	0.0567990000	-0.0623220000
C	1.6989550000	-2.9754650000	-0.0438480000
C	-0.8487190000	-3.3032960000	-0.0869630000
C	-2.1507640000	2.6152330000	0.1316640000
C	1.5426780000	3.2840420000	0.2250290000
C	-1.0175340000	3.4871360000	0.1935030000
C	-3.4135350000	-2.8783100000	-0.1008440000
F	-3.3131110000	0.0888210000	-1.2938210000
F	-3.5135690000	-0.0123710000	1.0177120000
H	2.2740920000	-2.5938840000	-0.8957010000
H	1.7120170000	-4.0700450000	-0.0901810000
H	2.2347000000	-2.6711810000	0.8629210000
H	-0.8364550000	-4.3837560000	-0.1099800000
C	-3.5578800000	2.9415450000	0.1377560000
H	2.0888270000	2.9349270000	1.1093070000
H	1.4997470000	4.3780590000	0.2672460000
H	2.1408480000	3.0017660000	-0.6492880000
H	-1.0582290000	4.5650430000	0.2604150000
C	4.7882380000	0.2572900000	0.0274540000
H	9.0096330000	2.2558330000	-3.5326380000
H	7.4992910000	-0.9022440000	-3.2992100000
C	-3.8361550000	-4.1778390000	-0.1527700000
C	-4.0385710000	4.2214270000	0.1688990000
H	-3.0853170000	-4.9686690000	-0.1832760000
H	-3.3232190000	5.0449700000	0.1794370000
H	-4.1352260000	-2.0692990000	-0.0667280000

H	-4.2415550000	2.0994760000	0.1202600000
C	-5.2232030000	-4.6437340000	-0.1703120000
C	-5.4812770000	-6.0412770000	-0.2220210000
C	-6.3414230000	-3.7716140000	-0.1359750000
C	-6.7840310000	-6.5463010000	-0.2374140000
H	-4.6427390000	-6.7347460000	-0.2491630000
C	-7.6536850000	-4.2630720000	-0.1506770000
H	-6.1899880000	-2.6966580000	-0.0969110000
C	-7.8788710000	-5.6574930000	-0.2007950000
H	-6.9795290000	-7.6135420000	-0.2757260000
H	-8.4832270000	-3.5640390000	-0.1231880000
C	-5.4442390000	4.6272680000	0.1897980000
C	-5.7610640000	6.0136300000	0.1969890000
C	-6.5241800000	3.7077200000	0.2081960000
C	-7.0837200000	6.4631510000	0.2206600000
H	-4.9526770000	6.7423770000	0.1839450000
C	-7.8560090000	4.1432940000	0.2336760000
H	-6.3268700000	2.6394900000	0.2057300000
C	-8.1396240000	5.5279500000	0.2403100000
H	-7.3244820000	7.5217870000	0.2265170000
H	-8.6555470000	3.4096590000	0.2490920000
O	-9.4248020000	6.0664550000	0.2666910000
O	-9.1408390000	-6.2488780000	-0.2173320000
C	-10.3257530000	-5.3927820000	-0.1669440000
H	-10.3266440000	-4.7905850000	0.7516270000
H	-10.3547310000	-4.7240910000	-1.0378330000
C	-10.5733030000	5.1620140000	0.3160710000
H	-10.5942640000	4.5170420000	-0.5727110000
H	-10.5310120000	4.5353520000	1.2171190000



C	-11.8065720000	6.0571810000	0.3534430000
H	-11.7670020000	6.7228950000	1.2297620000
H	-11.8588210000	6.6761910000	-0.5558340000
C	-11.5238530000	-6.3350140000	-0.1813880000
H	-11.4850160000	-7.0150200000	0.6839050000
H	-11.5261750000	-6.9383670000	-1.1026000000
O	-12.9497590000	5.1602140000	0.4367170000
O	-12.7016170000	-5.4821760000	-0.1172410000
C	-14.2330240000	5.8529750000	0.4877220000
H	-14.2704360000	6.5350660000	1.3514040000
H	-14.3934850000	6.4392080000	-0.4303760000
C	-13.9600320000	-6.2208060000	-0.1134610000
H	-14.0050000000	-6.9044600000	0.7485850000
H	-14.0652280000	-6.8116390000	-1.0366360000
C	-15.3058390000	4.7779430000	0.6209200000
H	-15.2676060000	4.0924870000	-0.2404330000
H	-15.1457220000	4.1936710000	1.5407930000
C	-15.0740320000	-5.1840950000	-0.0211150000
H	-14.9659570000	-4.5918930000	0.9012900000
H	-15.0299470000	-4.5000840000	-0.8833630000
O	-16.5836030000	5.4760340000	0.6681430000
O	-16.3280750000	-5.9253990000	-0.0144230000
C	-17.7307120000	4.5858720000	0.8091870000
H	-17.7835870000	3.8833180000	-0.0371400000
H	-17.6591200000	4.0055420000	1.7423180000
C	-18.9720590000	5.4706870000	0.8358210000
H	-18.9171660000	6.1761880000	1.6805960000
H	-19.0465460000	6.0491060000	-0.0991920000
C	-17.5086170000	-5.0727810000	0.0725470000

H	-17.4883010000	-4.4749860000	0.9971690000
H	-17.5557820000	-4.3863600000	-0.7872730000
C	-18.7203580000	-5.9980280000	0.0726640000
H	-18.6740070000	-6.6846000000	0.9333850000
H	-18.7414600000	-6.5968500000	-0.8521900000
O	-20.1114490000	4.5750890000	0.9826130000
O	-19.8928310000	-5.1379130000	0.1592420000
C	-21.3883650000	5.2664430000	1.0294400000
H	-22.1550420000	4.4951970000	1.1412680000
H	-21.4382140000	5.9588010000	1.8856420000
H	-21.5720600000	5.8330630000	0.1020010000
C	-21.1476260000	-5.8699280000	0.1754610000
H	-21.2061720000	-6.5461200000	1.0439280000
H	-21.9422850000	-5.1222590000	0.2435050000
H	-21.2793380000	-6.4608840000	-0.7456090000
C	11.9593000000	0.8433480000	-2.3773280000
C	12.4329730000	0.6319110000	-0.9506740000
H	12.0687790000	-0.3461150000	-0.6103590000
H	11.9327030000	1.3668640000	-0.3065560000
C	13.9629080000	0.7290370000	-0.8116180000
H	14.4397150000	-0.0038780000	-1.4764830000
H	14.3009260000	1.7174480000	-1.1523910000
C	14.4211010000	0.4905970000	0.6426960000
H	13.9441260000	1.2318980000	1.3038200000
H	14.0793990000	-0.5004750000	0.9720120000
C	15.9587650000	0.5877770000	0.7863890000
H	16.4376530000	-0.1618300000	0.1422180000
H	16.2861390000	1.5691300000	0.4155140000
C	16.4406900000	0.4309050000	2.2370690000

C	16.5601460000	-0.9894530000	2.8150870000
S	18.2948420000	1.0370700000	2.4675720000
C	17.8593960000	-1.6090710000	2.2444140000
C	18.9937640000	-0.7387280000	2.7749260000
H	19.9242210000	-0.8248770000	2.2100260000
N	15.6104600000	-2.0824250000	2.5466610000
N	17.6710700000	-3.0135560000	2.6376290000
H	14.6324670000	-2.0561870000	2.8070670000
H	18.3304920000	-3.7532470000	2.4310830000
C	16.2929830000	-3.3149250000	2.6322340000
O	15.7789420000	-4.4502450000	2.6899260000
H	17.8456240000	-1.5205210000	1.1458770000
H	16.6974830000	-0.8801390000	3.9057530000
O	12.7096300000	1.0739250000	-3.3438630000
H	15.8602740000	1.0784110000	2.9023810000
H	19.1706620000	-0.8808690000	3.8436110000

**Table S2.** Excitation energies and oscillator strengths obtained from TD-DFT calculations for complex **1**

Energy (eV)	$\lambda$ /nm	Oscillator strength (f)	Transition
1.6262	762	0.0005	HOMO→LUMO
1.9528	635	1.0366	HOMO→LUMO+2
2.2632	547	0.0000	HOMO-1→LUMO
2.5208	491	0.0035	HOMO-1→LUMO+1
2.6878	461	0.5022	HOMO-1→LUMO+2
2.7561	449	0.0000	HOMO-2→LUMO+1

## References

**S1.** A. D. Becke, *Phys. Rev. A: At. Mol., Opt. Phys.*, 1988, **38**, 3098-3100.

**S2.** A. D. Becke, *J. Chem. Phys.*, 1993, **98**, 5648–5662.